Oceanologia (2019) 61, 143—169

Available online at www.sciencedirect.com

ScienceDirect

journal homepage: www.journals.elsevier.com/oceanologia/

ORIGINAL RESEARCH ARTICLE

Average nutrient and chlorophyll distributions in the western Mediterranean: RADMED project

María del Carmen García-Martínez [a,*], Manuel Vargas-Yáñez [a], Francina Moya [a], Rocío Santiago [b], María Muñoz [c], Andreas Reul [c], Teodoro Ramírez [a], Rosa Balbín [b]

[a] *Instituto Español de Oceanografía, C.O. Málaga (Fuengirola), Spain*
[b] *Instituto Español de Oceanografía, C.O. Baleares, Spain*
[c] *Universidad de Málaga. Departamento de Ecología, Spain*

Received 31 May 2018; accepted 16 August 2018
Available online 2 September 2018

KEYWORDS
Inorganic nutrients;
Chlorophyll;
Western Mediterranean;
Climatological values;
Time series;
Climate change

Abstract Because of its reduced dimensions and its location, surrounded by three continents, the Mediterranean Sea could be especially vulnerable to climate change effects. An increase of the water column stratification could inhibit winter mixing and reduce the frequency and intensity of convection processes which inject nutrients into the photic layer and are responsible for the ventilation of deep waters. In this context, the long-term monitoring of the Mediterranean waters is a basic task. The RADMED project is a monitoring program that covers the waters from the eastern side of the Gibraltar Strait to the Catalan and Balearic Seas. This project was initiated in 2007, merging some previous programs, some of them initiated in 1992. The main objective of this project is to establish average distributions, ranges of variability and long-term trends for physical, and biochemical variables which could be considered as indicative of the environmental state of the sea. The present work analyses nutrient, chlorophyll and oxygen time series from 2007 to 2015 in some cases and from 1992 in other cases. The current analyses show a clear trophic gradient in the RADMED area. Nutrient and chlorophyll concentrations and the intensity of the deep chlorophyll maximum decrease northeastward. The deep chlorophyll maximum depth increases to the northeast. The Balearic and Catalan Seas show a clear seasonal pattern with maximum surface concentrations for nutrients and chlorophyll in winter/spring, associated with winter mixing. On the contrary, the Alboran Sea does not show such a clear seasonal cycle,

* Corresponding author at: Instituto Español de Oceanografía, Centro Oceanográfico de Málaga (Fuengirola), n/n, 29640 Fuengirola (Málaga), Spain.
E-mail address: mcarmen.garcia@ieo.es (M.d.C. García-Martínez).
Peer review under the responsibility of Institute of Oceanology of the Polish Academy of Sciences.

Production and hosting by Elsevier

https://doi.org/10.1016/j.oceano.2018.08.003

probably because of the existence of permanent upwelling processes acting along the whole year. The Atlantic Water occupying the upper part of the water column shows a Redfield N:P ratio close to or lower than 16, indicating no phosphorus limitation. Finally, chlorophyll concentrations seem to have increased from 1992 to 2015 in the Alboran Sea, while no long-term changes could be established for the rest of the variables and geographical areas.

1. Introduction

The Mediterranean Sea is characterized by an anti-estuarine circulation with fresh Atlantic Water (AW) flowing at the surface into the Mediterranean, and saltier Mediterranean Water outflowing at depth to the Atlantic. The surface AW has low nutrient concentrations while the Mediterranean Water (MW) shows higher values. The result is a net nutrient transport from the Mediterranean to the Atlantic and, as a consequence, the oligotrophic character of the Mediterranean Sea (Bethoux et al., 1998, 2002; D'Ortenzio and Ribera d'Alcala, 2009; Powley et al., 2017; Schroeder et al., 2010). This oligotrophy increases from west to east at the same time that phytoplanktonic biomass and the *f* ratio (new to total primary production) decrease (Bethoux et al., 1998; Estrada, 1996; Lavigne et al., 2015). This nutrient deficit is compensated by river runoff, atmospheric depositions and nitrogen-fixing organisms (Bethoux et al., 1998; Macías et al., 2014, 2018).

In spite of this general oligotrophy, the Mediterranean Sea is able to sustain moderate levels of primary production. This fact has been known as the "Mediterranean paradox" (Estrada, 1996; Sournia, 1973). The explanation seems to be a high regenerated production and the existence of several fertilizing mechanisms acting at some specific locations within the Mediterranean. These processes are: frontal and mesoscales structures responsible for an important vertical circulation, winter mixing (intermediate and deep convection) and nutrient inputs from such rivers as the Nile, Rhone, Po and Ebro. Furthermore, the AW flowing into the Western Mediterranean (WMED) is not as impoverished as previously thought. Intense current shear, internal tides and the upward displacement of the Atlantic-Mediterranean interface, from southwest to northeast at the Strait of Gibraltar, are able to inject nitrate and phosphate into the upper layer of the WMED (Echevarría et al., 2002; Gómez et al., 2000, Gómez, 2003; Huertas et al., 2012). These mechanisms would account for the difference between the oligotrophy of the WMED and the ultra-oligotrophy of the Eastern Mediterranean (EMED, Powley et al., 2017). The result of these different mechanisms is the existence of a complex distribution of trophic regimes, with some areas showing a behavior similar to that of sub-tropical regions and other ones closer to temperate zones (D'Ortenzio and Ribera d'Alcala, 2009).

As already commented, the distributions of nutrients, chlorophyll and dissolved oxygen (DO) are modulated by several processes and therefore can differ across the Mediterranean Sea. Nevertheless, some common features can be established. In the case of the WMED, nutrient concentrations at surface layers are very low during the stratified period (late spring to autumn) and increase to maximum values at the depth of the Levantine Intermediate Water (LIW, 200—400 m) with concentrations around 9.5 μM and 0.45 μM for nitrate and phosphate respectively. These concentrations then slightly decrease to the sea bottom (8.5 μM and 0.4 μM). Silicate concentrations simply increase with depth without any maximum at intermediate levels. This fact has been attributed to lower remineralization rates. An almost ubiquitous Deep Chlorophyll Maximum (DCM) is also observed for the stratified period at depths increasing from west to east. During the mixing period (late autumn to winter), surface nutrient concentrations increase and the position of the DCM is shallower or even disappears, being the maximum chlorophyll concentrations at the sea surface (Lavigne et al., 2015). DO is at saturation levels at the sea surface increasing to a maximum value linked to photosynthetic activity at the depth of the DCM or above it. The nutrient maxima at the LIW depth are also accompanied by a DO minimum. DO values increase to the sea bottom, as deep waters are well ventilated by winter deep convection processes occurring in the Northwestern Mediterranean.

The Mediterranean Sea has been considered as a sea "under siege" (Coll et al., 2011). Several anthropogenic stressors such as an increasing population at the coast or the increase of agriculture, industrial and tourism activities seem to threaten marine ecosystems enhancing phenomena such as eutrophication at some coastal areas (Macías et al., 2018). It has also been suggested that climate change could increase the vertical thermal stratification and/or increase the stratified period, decreasing the nutrient supply to the photic layer (Calvo et al., 2011). A similar effect would be expected from a reduction in the intensity and frequency of intermediate and deep convection which is responsible for the ventilation of deep waters and the injection of nutrients at the upper part of the water column. Some areas of the world ocean have already evidenced a reduction of the DO content associated with the solubility decrease of warming waters and the lower ventilation rates (Schmidtko et al., 2017).

Within this context, the monitoring of the biogeochemical properties of the Mediterranean waters becomes a basic task. Climatological values, variability ranges and the detection of possible trends is of prime importance for the detection and quantification of climate change and other anthropogenic effects. Beside this, routine time series of variables such as nutrients, chlorophyll-*a*, phyto- and zooplankton abundance, *etc*. could be beneficial for operational services (www.emodnet.eu, www.copernicus.eu). Nevertheless, oceanographic stations with periodic *in situ* sampling of biochemical variables are scarce. For the case of the WMED, one of the

longest open sea periodic stations is the Dyfamed station at the Ligurian Sea (Marty and Chiavérini, 2002, 2010; Pasqueron de Fommervault et al., 2015). Examples of coastal oceanographic stations are the Blanes Bay Microbial Observatory in the Catalan coast (see for instance Gasol et al., 2016) or those in the Italian RITMARE network (Ravaioli et al., 2018). General descriptions of the vertical and horizontal distributions of nutrient and chlorophyll-*a* concentrations have been obtained from the compilation of *in situ* measurements from oceanographic surveys (Manca et al., 2004) or from the analysis and inter-calibration of fluorescence profiles (Lavigne et al., 2015). Nevertheless, the information is scarce and unevenly distributed not allowing to obtain seasonal climatological profiles for some areas and some variables such as chlorophyll-*a* (Manca et al., 2004). In other cases, our knowledge about the seasonal dynamics of nutrients and phytoplankton communities do not derive from long-term time series, but from research projects covering just one seasonal cycle. Although very valuable information has been obtained, it seems to be unevenly distributed. A good example is the westernmost part of the Mediterranean Sea. A large amount of information is available for the continental shelf and slope of the Catalan Sea and the frontal zone at the Catalan shelf break (Estrada et al., 2014; Gasol et al., 2016; Latasa et al., 2010; 2016; Segura-Noguera et al., 2016). Similarly, a large number of surveys have described the nutrient, chlorophyll, phyto- and zooplankton communities and the primary production in the Alboran Sea (L'Helguen et al., 2002; Morán and Estrada, 2001; Ramírez et al., 2005; Reul et al., 2005), paying special attention to the upwelling areas in the Northwestern Alboran Sea and the Almería-Orán front. On the contrary, biogeochemical information from the Balearic Sea, the Balearic front, and mainly the eastern coast of the Spanish Mediterranean, from the north of Cape Gata to Valencia Gulf is very sparse.

One attempt to fill these gaps corresponds to the RADMED program from the Instituto Español de Oceanografía (Spanish Institute for Oceanography). This project is devoted to the implementation and maintenance of a monitoring system around the continental shelf and slope, including some deep stations (>2000 m) around the Spanish Mediterranean (López-Jurado et al., 2015; Tel et al., 2016). It is aimed at the study of the seasonal and long-term variability of the westernmost Mediterranean waters from a multidisciplinary point of view. Oceanographic stations are visited on a seasonal basis since 1992 in some cases and since 2007 in the case of the stations most recently included in the RADMED project. Garcia-Martinez et al. (2018), Vargas-Yáñez et al. (2017) have shown that temperature and salinity data from the RADMED project can be merged with historical data in order to construct long time series. These works updated temperature and salinity time series by extending the previous ones to 2015 (inclusive). The goal of the present work is to complete the hydrological information presented in previous works with nutrient, chlorophyll and DO distributions along the RADMED area. In some cases, the length of the time series will allow us to establish climatological profiles and ranges of variability as well as linear trends which could be used as a reference for future works and operational services. In other cases, the oceanographic stations have been initiated very recently and they will simply be used as a first attempt to estimate the average seasonal cycles of nutrient, chlorophyll and DO concentrations, relating them to the physical forcing and general circulation of the WMED. Section 2 presents the data set, Section 3 shows the main results, and a discussion and summary are presented in Section 4.

2. Data and methods

The RADMED project is a monitoring program funded by the Instituto Español de Oceanografía. This program was launched in 2007, unifying and extending previous monitoring programs: ECOMÁLAGA, initiated in 1992 in the area of the Málaga Bay, ECOBALEARES, initiated in 1994 to the south of Mallorca Island, and ECOMURCIA and CIRBAL to the south of Cape Palos and in the Balearic Channels respectively, initiated in 1996 (Fig. 1). The stations are distributed in transects perpendicular to the coast, covering the continental shelf and slope and in some cases some deep stations (>2000 m). Stations are named by a letter corresponding to each transect and a number increasing from the coast to the open sea. In the Alboran Sea, the westernmost transects are Cape Pino (P in Fig. 1), Málaga (M) and Vélez (V). For instance, the closest station to the coast in Cape Pino transect is named as P1, and the most offshore station is P4. Sacratif transect extends from Cape Sacratif in the central part of the Alborán Sea, and Cape Gata transect (CG) is on its eastern limit. Those transects extending from the eastern Spanish coast are Cape Palos (CP), Tarragona (T) and Barcelona (BNA). Two more transects are located in the Balearic Islands, one of them to the south of Mallorca Island (B) and another one extending in a northeast direction from Menorca Island (MH). 37 oceanographic stations forming two triangles cover the Balearic channels: The Ibiza channel between the peninsula and Ibiza Island and the Mallorca channel between Ibiza and Mallorca. These stations are labelled as C. Finally a deep station (>2200 m) is located to the south of Cabrera Island (EPC). All the stations are visited three-monthly, that is, once per season, unless weather conditions or technical problems prevent the sampling.

CTD profiles are obtained in all the stations. The hydrographic sampling is done using CTDs, mainly model SBE 911 and as spare instruments, the models SBE 25 or SBE 19+, installed in a carousel water sampler SBE 32. CTDs are equipped with a Dissolved Oxygen SBE 43 sensor. DO and conductivity sensors are calibrated using water samples for selected depths of the water column at least once for a campaign, when it lasts less than a week, and at least at the beginning and at the end of the campaign, when it is longer. The DO determinations to calibrate the SBE 43 sensor are performed by the Winkler titration method (Strickland and Parsons, 1972) and by direct spectrophotometry of total iodine at 456 nm (Labasque et al., 2004; Pai et al., 1993). The salinity calibrations are done using a Guildline 8400 Autosal.

Water samples for the determination of nutrients and chlorophyll-*a* are taken at all the stations. Water samples for nutrient determinations are taken at 0, 10, 20, 50, 75, 100, 200, 300, 500, 700, 1000 m, and sea bottom for deep stations while sampling is limited to the station depth for the shallower ones. Nutrient samples are collected using 12 ml vials that are kept frozen at −20°C until they are analyzed in the laboratory. Nitrate, nitrite and silicate concentrations

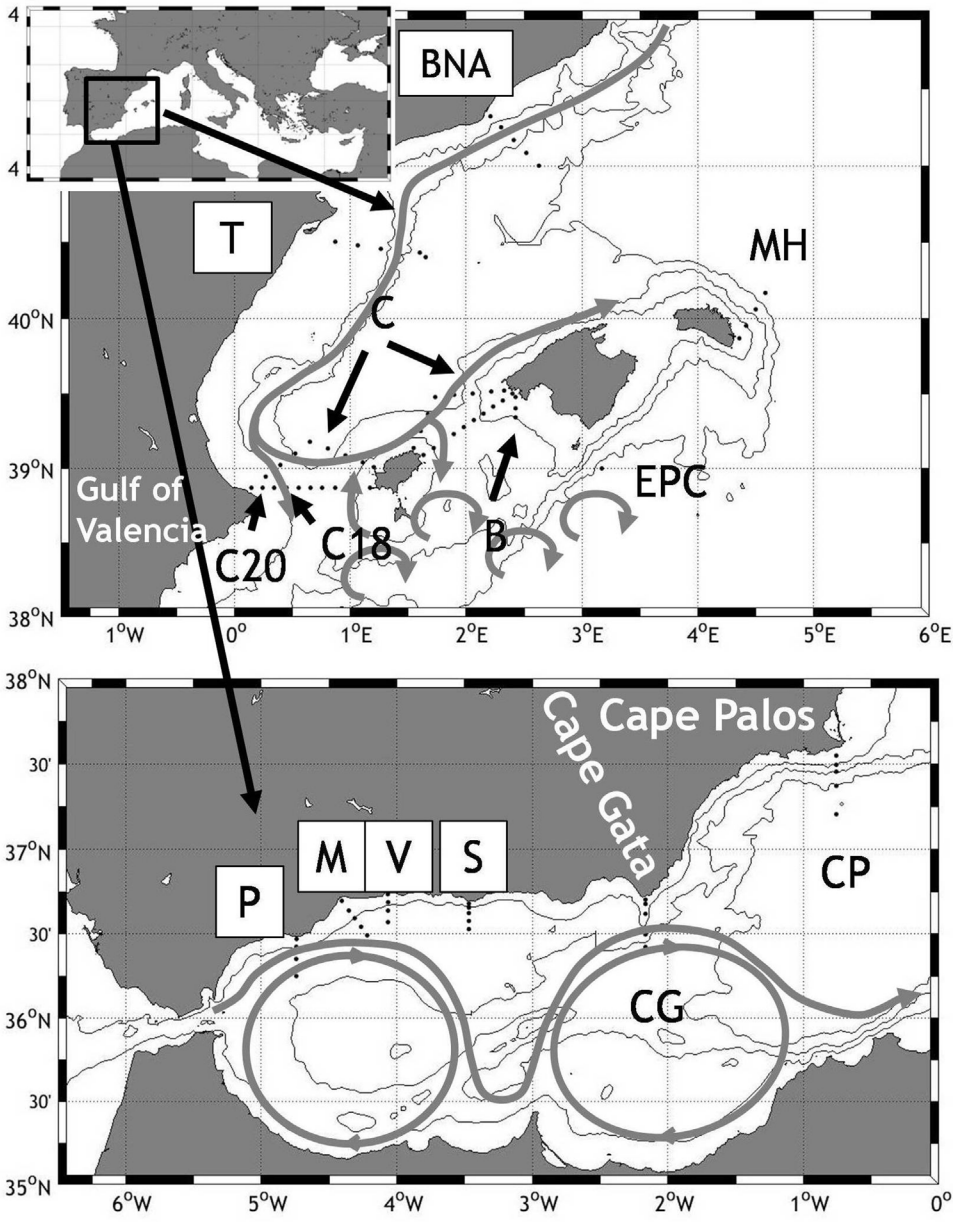

Fig. 1 RADMED area within the Western Mediterranean. The upper map shows the northern RADMED stations. The lower map shows the Alboran Sea and Cape Palos RADMED stations. The labels for each transect are included. Stations C20 (continental shelf) and C18 (continental slope) from the Ibiza Channel are also indicated. 200, 500 and 1000 m isobaths have been included. The grey line shows a schematic of the AW circulation.

are determined according to the methods in Grasshof et al. (1983). Phosphate concentrations are determined by the method of Treguer and Le Corre (1975). All these methods are adapted to oligotrophic waters and analyses are performed with a Technicon Autoanalyzer AAIII and QuAAtro Marine of SEAL 25 Analytical. Samples for chlorophyll-*a* determinations are limited to the upper 100 m of the water column (0, 10, 20, 50, 75 and 100 m), or to the maximum depth for shallower stations. 1 l samples are filtered and kept frozen at −20°C until they are analyzed by fluorometry (Holm-Hansen et al., 1965) using a Turner 10 AU spectrofluorometer previously calibrated with pure chlorophyll-*a*.

For each transect, stations labelled as 2 are considered as representative of the continental shelf conditions and stations 4 represent the continental slope. Stations 2 are located over a bottom depth ranging from 75 to 295 m with most of the stations over 75 m depth. Stations labelled as 4 are at the continental slope with bottom depths ranging from 300 to 2500 m. For the triangles covering the Balearic Channels, stations C20 and C18 were chosen as representative of the peninsular continental shelf and slope conditions respectively (see Fig. 1). Table 1 shows the position, initial time, depth and sampling depths of stations labelled as 2 and 4. Protocols and further details about the sampling and data analysis can be

Table 1 Columns 1—4 show the positions for the stations labelled as 2 (continental shelf) and 4 (continental slope). Column 5 and 6 are the station name and depths respectively. Column 7 is the year when the sampling was initiated and column 8 shows the discrete depths where nutrients and chlorophyll is sampled.

Longitude (degrees)	Longitude (minutes)	Latitude (degrees)	Latitude (minutes)	Station	Depth	Initial year	Sampling depths
1	2	3	4	5	6	7	8
−4	−44.4960	36	25.4280	P2	130	1992	0-10-20-50-75-100-bottom
−4	−44.4960	36	15.0000	P4	870	2007	0-10-20-50-75-100-200-300-500-bottom
−4	−21.2160	36	38.3160	M2	75	1992	0-10-20-50-75
−4	−15.8280	36	32.5380	M4	350	2000	0-10-20-50-75-100-200-bottom
−4	−3.8460	36	41.2500	V2	75	1992	0-10-20-50-75
−4	−3.9000	36	34.2000	V4	490	2000	0-10-20-50-75-100-200-300-bottom
−3	−28.0920	36	39.3480	S2	300	2007	0-10-20-50-75-100-200-300
−3	−28.0920	36	34.6140	S4	650	2007	0-10-20-50-75-100-200-300-500-bottom
−2	−9.9120		40.6500	CG2	75	2007	0-10-20-50-75
−2	−9.9120	36	29.8260	CG4	700	2007	0-10-20-50-75-100-200-300-500-700
0	−45.4500	37	29.7900	CP2	75	2007	0-10-20-50-75
0	−45.4500	37	22.3680	CP4	2100	2003	0-10-20-50-75-100-200-300-500-700-1000-bottom
2	25.6020	39	28.6020	B1	75	1994	0-25-50-75
2	25.6020	39	24.1020	B2	100	1994	0-25-50-75-100
2	25.6020	39	20.5020	B3	200	1994	0-25-50-75-100-200
0	27.0000	38	52.2000	C18	300	1999	0-25-50-75-100-200-300
0	14.5980	38	52.2000	C20	95	2002	0-25-50-75-bottom
4	25.0020	39	57.0000	Mh2	180	2007	0-25-50-75-100-bottom
4	34.9620	40	10.0020	Mh4	2500	2007	0-25-50-75-100-200-300-500-700-1000-1500-bottom
1	3.8820	40	28.7700	T2	75	2007	0-10-20-50-75
1	36.0000	40	25.9020	T4	950	2007	0-10-20-50-75-100-200-300-500-700-bottom
2	18.1320	41	15.0000	BNA2	295	2007	0-10-20-50-75-100-200-bottom
2	31.1700	41	4.9980	BNA4	1320	2007	0-10-20-50-75-100-200-300-500-700-1000-bottom

seen in López-Jurado et al. (2015) or in www.repositorio.ieo.es/e-ieo/handle/10508/1762. The present work will be mainly focused on the analysis of stations 2 and 4. Additionally, stations P3, M3, V3 and CP3 over the shelf break will be analyzed because of its length and good temporal coverage.

All the individual profiles (four per year when there were no missing values) were grouped by seasons: winter (January—March), spring (April—June), summer (July—September) and autumn (October—December). Average profiles were calculated for each season for potential temperature, salinity, nitrate, nitrite, phosphate, silicate, DO and chlorophyll-*a*. Notice that nutrient and chlorophyll-*a* profiles were calculated at discrete depths.

The mixed layer depth (MLD) was calculated for each individual profile using both the maximum curvature criterion (Lorbacher et al., 2006) and the threshold method (De Boyer Montégut et al., 2004). After comparison of both methods, the latter was selected. The MLD was considered as that where the temperature was 0.3°C lower than a reference value that was considered as the temperature at 10 m depth. Once the MLD was determined for each temperature profile, the values were seasonally grouped and the average MLD was obtained for each season. A similar calculation was carried out for the nutricline which was considered as the depth where nitrate plus nitrite exceeded 1 μM (Macias et al., 2008). Secchi disk measurements were also obtained at stations 2 and 4 for each transect. Values for each station were also grouped by season and the average seasonal cycle was obtained.

The seasonal cycle for all the variables analyzed is made of four values corresponding to the winter, spring, summer and autumn mean values. These seasonal cycles were subtracted to the initial time series for obtaining time series of residuals or deviations. Such residuals time series were used for the estimation of decadal changes.

3. Results

3.1. Distribution of water masses

Fig. 2A shows the potential temperature-salinity (θS) diagrams for the Gulf of Cadiz, close to the Strait of Gibraltar and the θS diagrams for the continental shelf (Fig. 2B, C) and continental slope stations (Fig. 2D, E) in the RAMED area (hereafter it will always be written temperature for brevity but potential temperature is always used). The θS diagram for the Gulf of Cadiz shows the water mass flowing into the Mediterranean Sea. This figure is included in order to show the continuous modification of the waters occupying the upper layer (0—150 m) of the Mediterranean Sea. Differences between the θS diagrams in the RADMED stations and the properties of the water masses in the Gulf of Cadiz provide information about the degree of mixing with the underlying Mediterranean waters. The winter inflow corresponds to the upper part of the North Atlantic Central Water (NACW). The maximum depth of Camarinal Sill in the Strait of Gibraltar

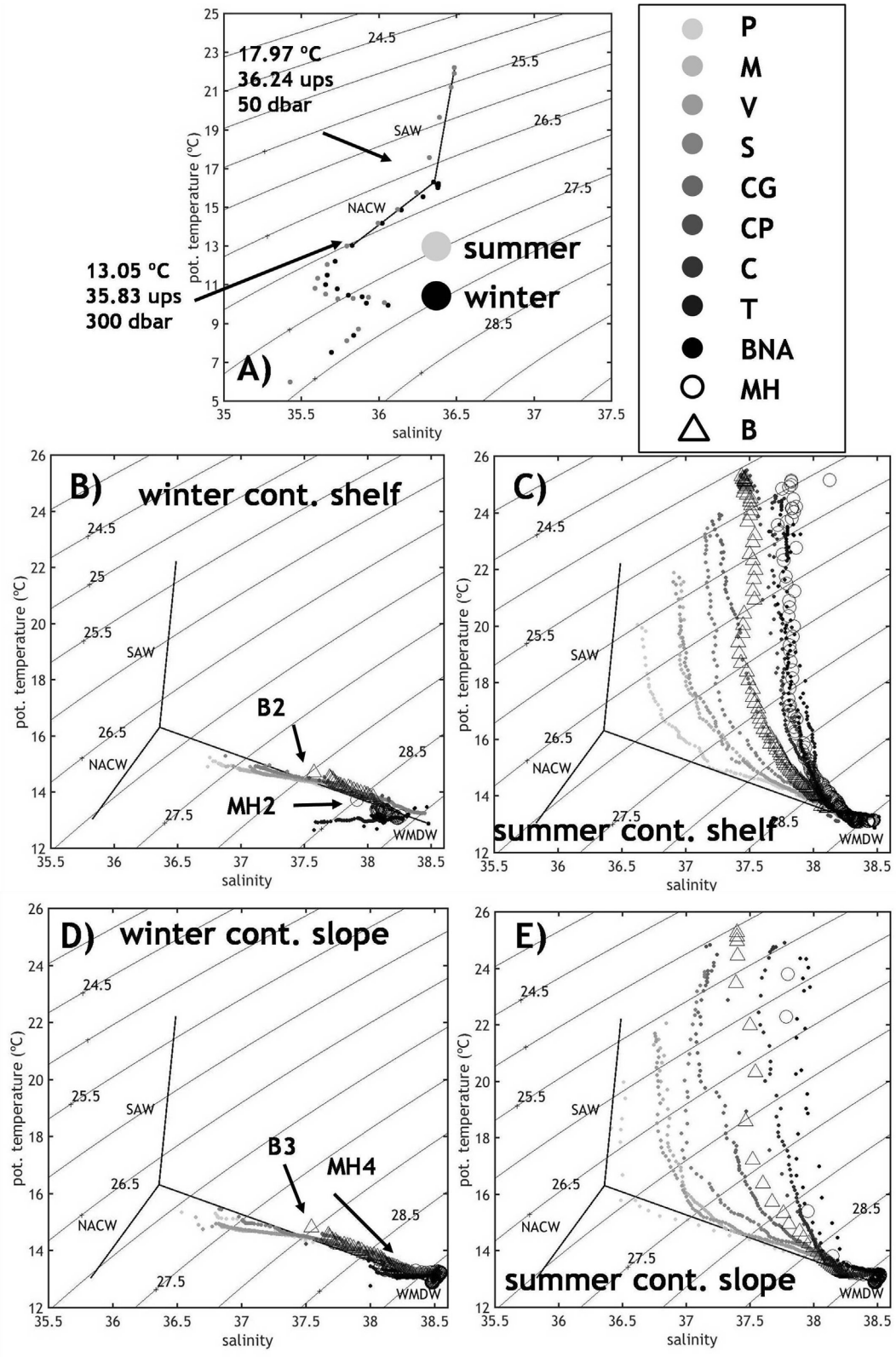

Fig. 2 Figure A shows the θS diagram for summer and winter in the Gulf of Cádiz, close to the eastern side of the Gibraltar Strait. Light grey dots are for summer and black ones for winter. Strait lines show the North Atlantic Central Water from the depth where summer heating is observed to 300 m, which is the maximum depth of the sill at Gibraltar. Waters above the NACW are labeled as Surface

limits the depth of the water column which is suitable for feeding the Atlantic current. This depth is around 300 m. The upper 300 m of the NACW is indicated at Fig. 2A as a continuous line. Fig. 2B to E use the same colour criterion. Grey dots are darker as the stations are further from Gibraltar. That is, light grey is used for stations close to the Strait of Gibraltar and black dots are used for the Barcelona stations (BNA). Winter diagrams (Fig. 2B and D) simply reflect that the water masses along the water column relay along the mixing line between the NACW and the Mediterranean Waters (Western Mediterranean Deep Water, WMDW and Levantine Intermediate Water, LIW). As the distance from Gibraltar increases (darker dots) the surface temperature and salinity are more different from the Atlantic values, indicating a higher percentage of Mediterranean waters. In all the stations this percentage increases with depth. Summer θS values (Fig. 2C, E) are similar to those for winter with the exception of the warming of the upper part of the water column, which is reflected in the almost vertical part of the diagram. Insular stations (MH and B) to the northeast of Menorca Island and to the south of Mallorca Island are represented by open circles and triangles respectively. The temperature and salinity values to the south of Mallorca seem to be similar to those of the peninsular side of the Ibiza Channel (stations C20, C18) at the same latitude, while Mahon (MH) properties resemble those of the northern stations T and BNA (Tarragona and Barcelona). The initial part (sea surface) of the B and MH θS diagrams are marked in Fig. 2 for the clarity of the plot. It is interesting to notice the low temperatures during winter in Barcelona continental shelf ($<13^{\circ}C$) with salinity values around 37.5 at the sea surface. This fact is the consequence of intense winter cooling and the possible influence of continental waters. These values suggest the Western Intermediate Water (WIW) formation in the Catalan shelf (López-Jurado et al., 1995; Vargas-Yáñez et al., 2012). Continental slope stations for Barcelona, Tarragona and Mahon (BNA, T and MH) show winter, spring (not shown) and summer temperatures below 13°C above the LIW temperature and salinity maxima. This indicates the presence of WIW. In summary, the net of oceanographic stations in the present work reflects the Atlantic-Mediterranean gradient of water masses within the WMED and some of the winter convection process occurring in the Northwestern Mediterranean.

3.2. Nutrients, dissolved oxygen and chlorophyll-*a* profiles

Chlorophyll-*a*, nutrient and DO average vertical profiles showed some common features for the whole sampling area, as well as some important differences. Figs. 3—8 show these average seasonal profiles for some selected stations. Confidence limits have not been included in these figures for the clarity of the plot. Nevertheless, one of the goals of this work is to provide mean values and ranges of variability which could be used as a reference for future works. Because of the huge amount of information, tables showing the average values, the standard deviations and the number of data used for the calculations are presented in the supplementary material (Table S1). Among the most recurrent features, it can be established that surface nitrate and phosphate concentrations are maxima in winter and/or spring and decrease for the summer season. For all the seasons, nitrate and phosphate concentrations increase with depth to a maximum located between 200 and 500 m, coinciding with the LIW depth level (see Figs. 4 and 6) and then slightly decrease with depth to the sea bottom. Chlorophyll-*a* concentrations reach maximum values in winter/spring when the surface waters have higher nutrient concentrations. Chlorophyll concentrations decrease during the stratified seasons, mainly summer and autumn. The depth where such a maximum is reached also increases from winter/spring, when it can be situated at the sea surface or at a sub-surface position (10—20 m), to summer and autumn, when the maximum chlorophyll concentrations deepen to 50—75 m, developing a Deep Chlorophyll Maximum (DCM) at some stations. Nitrite concentrations show an almost ubiquitous deep maximum usually found at or below the DCM. This maximum is usually referred to as Primary Nitrite Maximum (PNM, Lomas and Lipschultz, 2006). DO is at saturation at the sea surface increasing below the surface to a maximum at or above the DCM. When the maximum chlorophyll concentrations are at the sea surface, the highest DO values are also found at the sea surface (see Figs. 3 and 5A). DO decreases to a minimum at the LIW level and then increases to the sea bottom (Figs. 4 and 6).

In spite of these common features, the RADMED data show also important differences from the southwest to the northeast of the sampling area, and also between peninsular and insular waters. In the Alboran Sea, the highest chlorophyll concentrations are observed in winter in most of the Western Alboran Sea stations (P, M and V2) while such maximum values are advanced to autumn is the Eastern Alboran Sea (stations V4, S and CG, see Figs. 4A and 5D, 6D or chlorophyll concentrations at P2, P4, M2, M4, V2 and V4, S4, CG2, CG4 in Table S1). When the maximum chlorophyll concentrations correspond to winter, the lowest ones are observed in summer (western sector, P, M and V2) while, when maximum values correspond to autumn, the weakest chlorophyll concentrations are also moved forward to spring (eastern stations, S4, CG, Figs. 5 and 6). The maximum values of chlorophyll concentrations in the Western Alboran Sea occur at the sea surface or at 10—20 m depth (Tables 2—5). Therefore it is not properly a Deep Chlorophyll Maximum and the term sub-surface chlorophyll maximum is a more appropriate one. The intensity of the DCM (or sub-surface in the case of the Western Alboran Sea) also exhibits a SW-NE gradient. The highest DCM values are always higher than 1 mg/m^3 in the P, M, V and S stations. The chlorophyll concentrations within the weakest DCM of the year are higher than 0.5 mg/m^3. From CG transect to the east and north, the highest DCM values never exceed

Atlantic Water. Figures B and C show the θS diagrams for the continental shelf stations (labelled as 2 in each transect). Dots correspond to the peninsular continental shelf. A grey scale is used with the lightest grey for the P2 station, and darker grey as the distance to the Strait of Gibraltar is increased. Black dots correspond to BNA station. Open circles and triangles are for the MH and B stations respectively. Figures D, E are the same as figures B, C, but for the continental slope stations (labelled as 4).

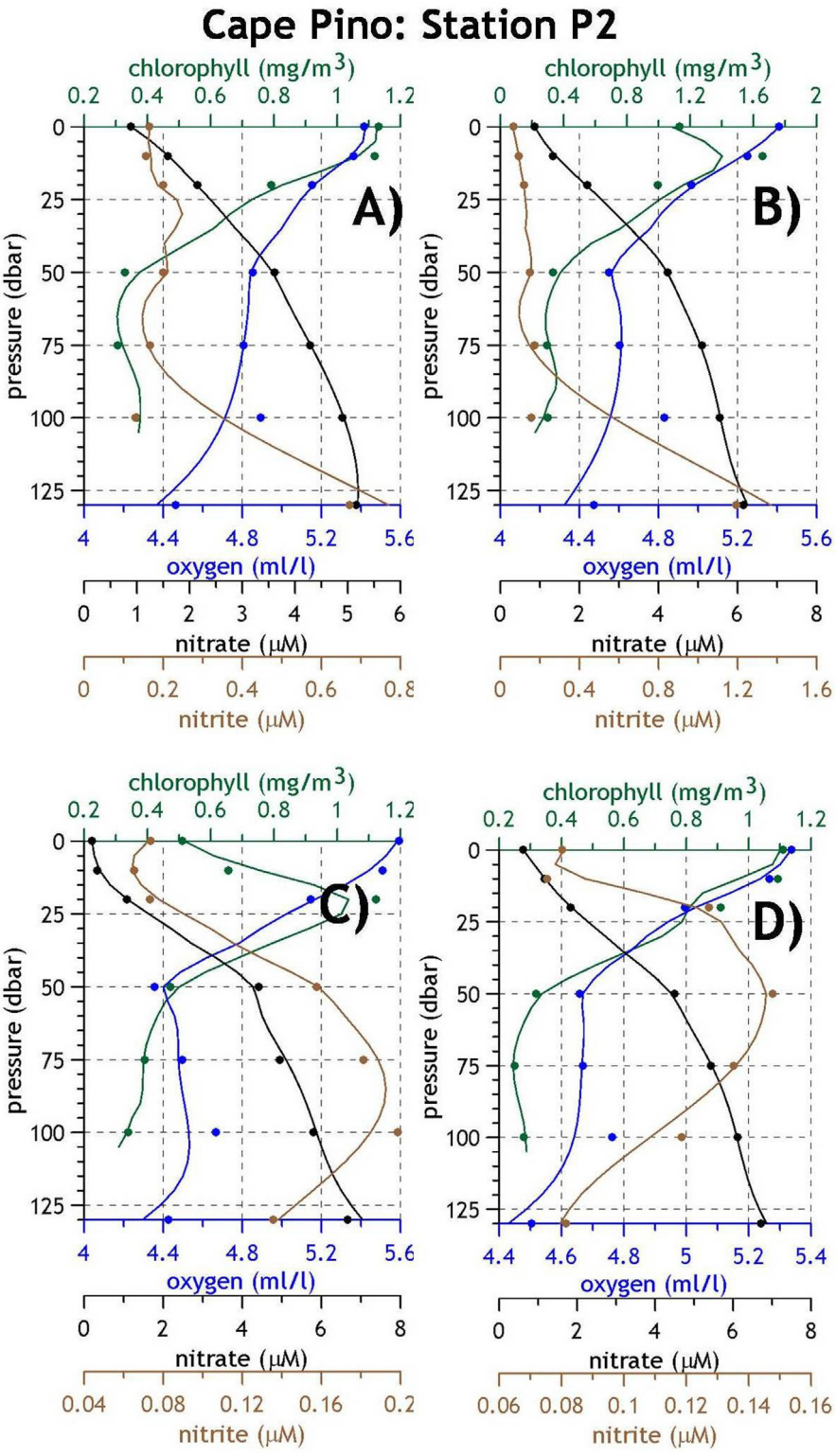

Fig. 3 Station P2, Cape Pino transect. Chlorophyll-*a*, nitrate, nitrite and DO average seasonal profiles. (A) Winter, (B) Spring, (C) Summer, (D) Autumn.

1 mg/m^3. Furthermore, the maximum DCM for CG, Cape Palos (CP) and Mallorca transect (B) is lower than 0.5 mg/m^3, that is, the maximum DCM is lower than the minimum ones in the Western Alboran Sea. The highest and lowest values of the DCM are reached in autumn and spring respectively in CG and CP. For the rest of the stations to the north of Cape Palos (C, T, BNA, B and MH), the highest values occur in winter/spring (Tables 2 and 3) and the lowest ones in summer/autumn (Tables 4 and 5). Another difference is observed for the depth of the DCM. For the case of the

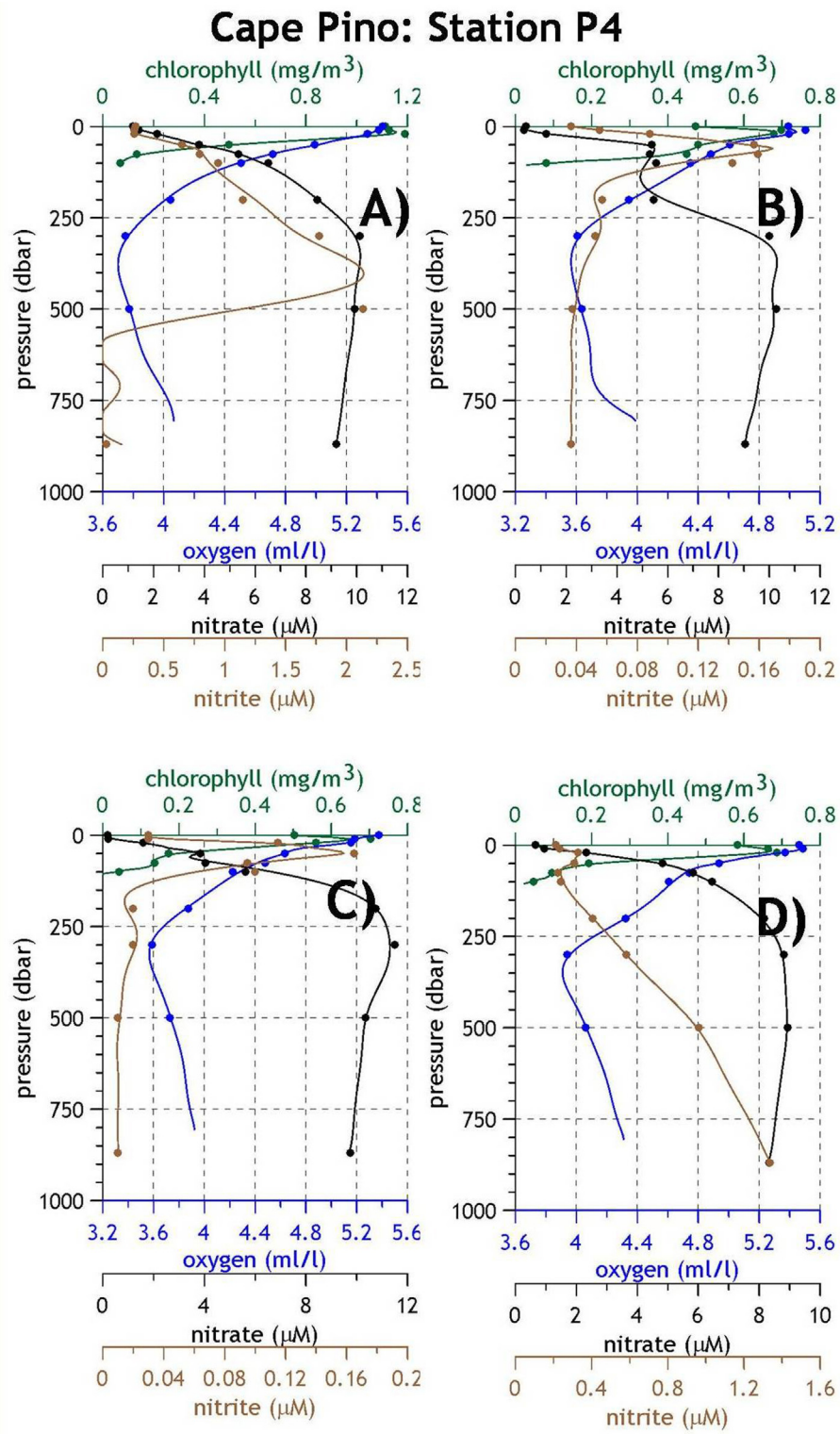

Fig. 4 Station P4, Cape Pino transect. Chlorophyll-*a*, nitrate, nitrite and DO average seasonal profiles. (A) Winter, (B) Spring, (C) Summer, (D) Autumn.

Western Alboran Sea (P, M and V) the highest chlorophyll concentrations are always at the upper 20 m of the water column. From S and CG (Alboran Sea) to the north, the DCM is at the upper 20—25 m when the highest concentrations are observed (mainly winter and spring) and it deepens to 50—75 m for the weakest summer and autumn values and even deeper (100 m) in the Mallorca transect (B2). Figs. 3 and 4 (stations P2 and P4) are shown as an example

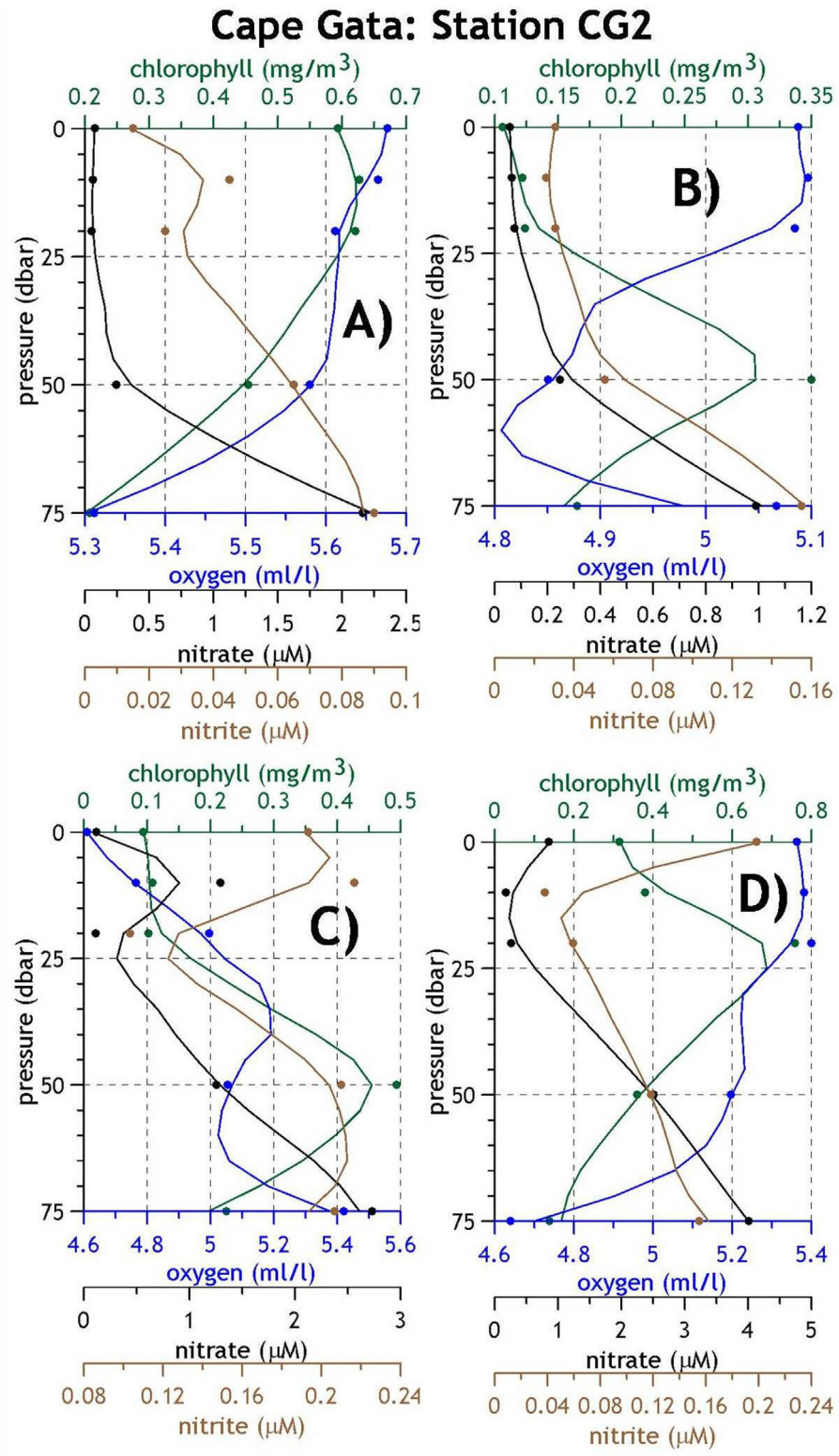

Fig. 5 Station CG2, Cape Gata transect. Chlorophyll-*a*, nitrate, nitrite and DO average seasonal profiles. (A) Winter, (B) Spring, (C) Summer, (D) Autumn.

of those stations within the Alboran Sea with high chlorophyll values during the whole year and maximum chlorophyll values at shallow waters or even at the sea surface. Figs. 5 and 6 (GC2 and CG4) are used as an example of weak and deeper DCM, and Figs. 7 and 8 are representative of very low chlorophyll concentrations with maximum values lower than 0.5 mg/m^3 (the autumn DCM is only 0.3 mg/m^3 at the B transect, Table 4).

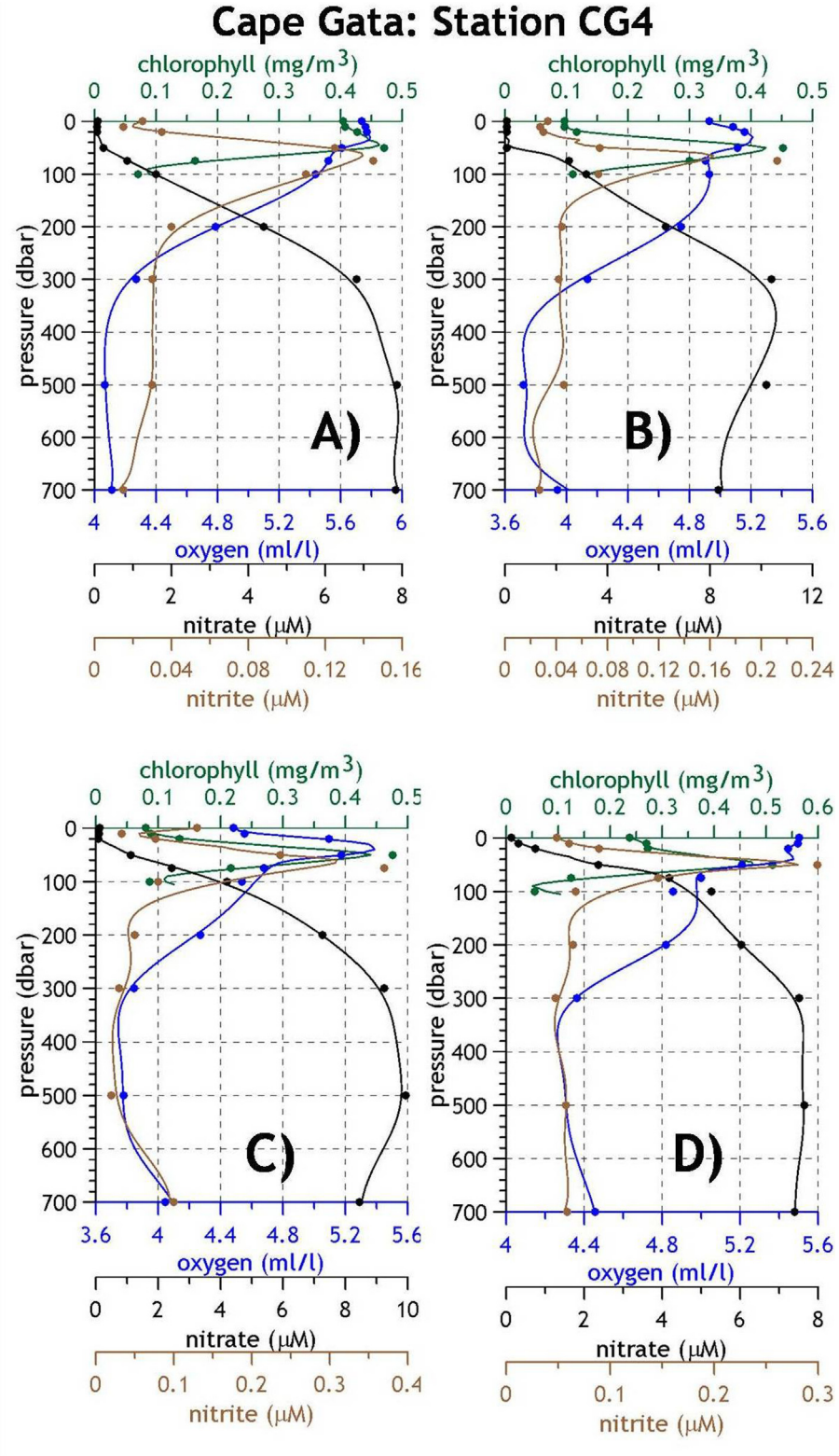

Fig. 6 Station CG4, Cape Gata transect. Chlorophyll-*a*, nitrate, nitrite and dissolved oxygen average seasonal profiles. (A) Winter, (B) Spring, (C) Summer, (D) Autumn.

Surface DO concentrations exhibit a clear seasonal cycle with minimum values in summer, when the temperature is higher and the solubility decreases. Nevertheless, stations P2, P4 and M2 are exceptions to this general behavior. The lowest DO concentrations associated to the nutrient maxima are at 300 m for the westernmost station P4. For M and V transects the minimum of DO is at the sea bottom as these stations

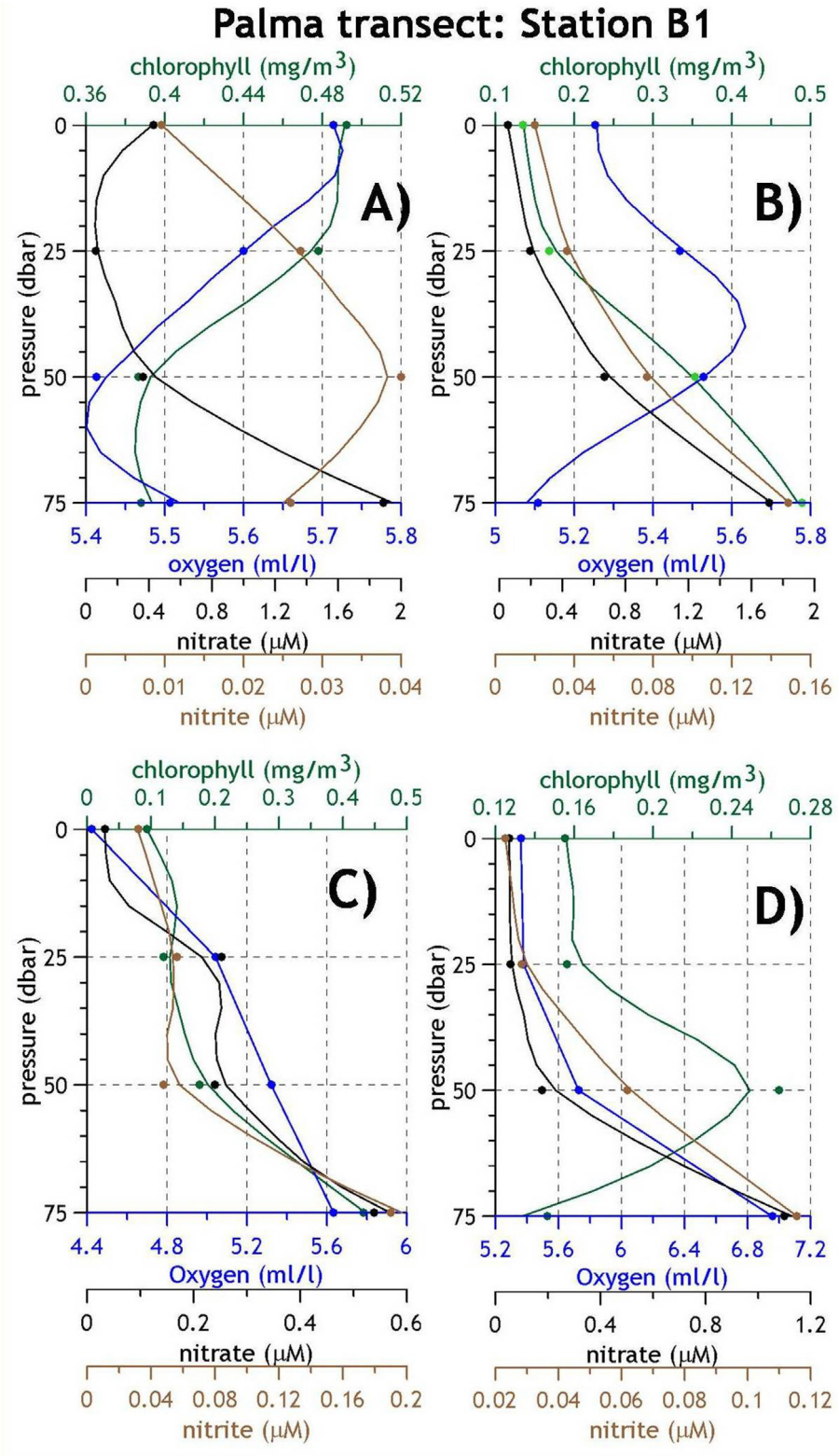

Fig. 7 Station B1, Mallorca transect. Chlorophyll-*a*, nitrate, nitrite and dissolved oxygen average seasonal profiles. (A) Winter, (B) Spring, (C) Summer, (D) Autumn.

are shallower than 500 m. For the peninsular and insular continental slope, from the S transect in the central Alboran Sea to the North, the DO minimum is almost always located at 500 m depth when the stations are deeper than this level. The DO minimum level is lower than 4 ml/l in the Alboran Sea with values close to 3.6 ml/l in the north of Cape Gata (Table S1).

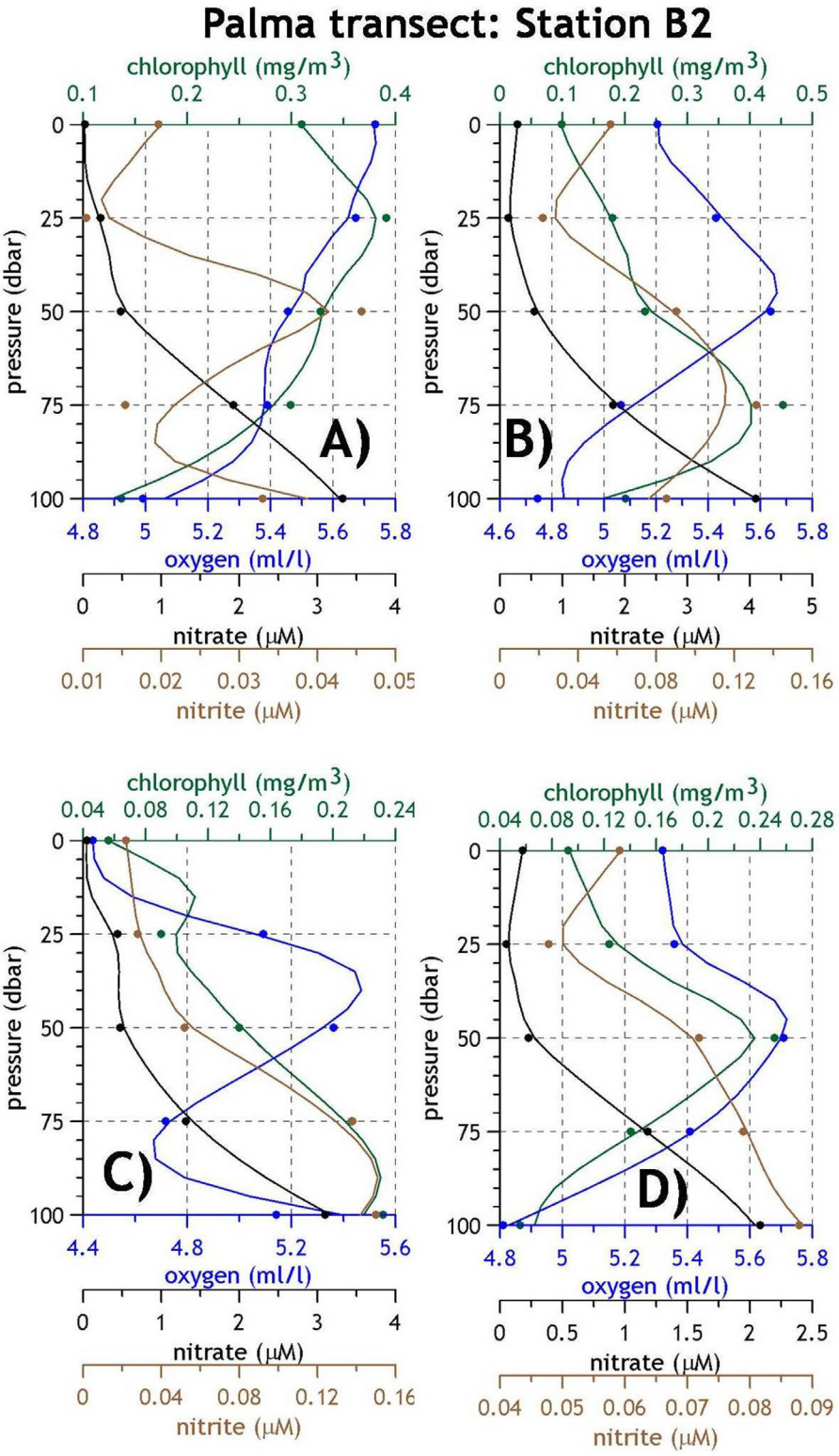

Fig. 8 Station B2, Mallorca transect. Chlorophyll-*a*, nitrate, nitrite and dissolved oxygen average seasonal profiles. (A) Winter, (B) Spring, (C) Summer, (D) Autumn.

Table 2 WINTER. Mixed layer depth (MLD), nutricline depth, integrated nitrogen (nitrate + nitrite), phosphate and silicate, integrated Dissolved Oxygen and chlorophyll, Deep Chlorophyll Maximum (DCM) concentration and depth and Secchi disk depth.

Winter	MLD (m)	Nut. Depth (m)	Int. N. (mmol/m)	Int. P. (mmol/m^2)	Int. Si. (mmol/m^2)	Int.DO. (L/m^2)	Int. Chl. (mg/m^2)	DCM (mg/m^3)	DCM Depth (m)	Secchi (m)
P2	56	13	291	19	223	495	53	1.4	6	14
P3	50	14	313	21	229	421	44	1.5	17	
P4	84	5	395	20	238	499	58	1.5	5	16
M2	58	14	160	12	138	380	58	1.4	15	13
M3	75	26	199	18	179	440	53	1.4	15	
M4	64	17	238	9	200	508	88	2.1	13	13
V2	52	16	176	12	140	382	59	1.5	20	13
V3	50	18	223	18	194	440	57	1.5	12	
V4	56	22	221	12	188	517	79	1.8	24	16
S2	40	0	315	20	229	504	60	1.1	22	18
S4	52	0	199	12	176	508	59	1.1	18	16
CG2	67	60	40	4	74	411	33	0.6	23	14
CG4	62	78	59	4	101	563	31	0.7	30	16
CP2	53	27	80	3	85	393	23	0.4	28	19
CP3	57	60	118	6	130	540	22	0.6	34	
CP4	84	34	197	7	132	483	33	0.7	33	16
C20	59	40	95	5	60	525	35	0.5	39	15
C18	153	41	148	6	128	553	28	0.4	36	19
T2	49	20	108	6	108	429	38	0.8	14	16
T4	190	55	109	4	156	558	38	0.5	32	18
BNA2	219	43	96	3	89	563	49	0.7	21	16
BNA4	870	0	184	5	175	526	39	0.7	31	18
B1	54	57	42	1	93	395	33	0.7	41	23
B2	56	58	122	1	138	509	31	0.6	42	23
B3	69	56	126	1	141	530	25	0.5	53	22
MH2	158	5	173	4	171	540	33	0.7	25	17
MH4	268	0	247	7	186	545	32	0.7	20	15

3.3. Mixed layer depth and nutricline. Integrated nutrients, chlorophyll-*a* and dissolved oxygen

MLD, nutricline depth, DCM concentration and depth, and chlorophyll-*a*, nitrogen (nitrate + nitrite), phosphate and silicate integrated concentrations from the surface to 100 m depth were calculated. The seasonal average values for all the RADMED stations are presented in Tables 2—5. In addition, Secchi disk depths have been included (see Table S2 for the complete statistics of the Secchi disk). Figs. 9A, B to 11A, B show the MLD (dashed black line), the DCM depth (continuous black line), DCM concentration (purple line) and integrated chlorophyll-*a* (dark green bars). Figs. 9C, D to 11C, D show the nutricline depth (dashed black line), integrated nitrate (white bars), integrated silicate (continuous black line) and integrated phosphate (dark brown bars). Figs. 9E, F to 11E, F show the integrated DO (dark blue bars), depth of the DO maximum (continuous black line), DO maximum concentration (continuous light blue line), depth of the DO minimum (dashed black line) and the DO minimum concentration (dashed light blue line).

P2 and P4 stations at the westernmost section of the RADMED area show a MLD (dashed line in Fig. 9A, B) which is maximum in winter (60 and 80 m respectively) and minimum in summer when the water column has a stronger stratification (~10 m). At station P4, Chlorophyll-*a* integrated for the upper 100 m of the water column is maximum for the same season when the MLD reaches its highest value and then decreases as the MLD becomes shallower. The behavior of the chlorophyll concentration at the DCM also follows that of the MLD at station P4. On the contrary, this relationship is not so clear in station P2 where weak values of the DCM concentration are coincident with high integrated chlorophyll values in winter. The depth of the nutricline (dashed lines in Figs. 9C, D to 11C, D), shows the lowest values (shallowest position) in winter at stations P2 and P4 (Fig. 9) while it is at the deepest levels (maximum values) during summer. Therefore MLD and nutricline show opposite seasonal patterns. Nitrogen (nitrate plus nitrite), phosphate and silicate concentrations integrated for the upper 100 m of the water column do not seem to follow the mixed layer and nutricline patterns, with the only exception of station P4 (Fig. 9D). Integrated DO seems to respond to the MLD and nutricline seasonal patterns with lowest values in summer when the MLD is shallower and the nutricline is at its deepest level.

Although the seasonal cycle of integrated variables does not show a common pattern, it can be observed the southwest-northeast gradient already described for the surface nutrient concentrations and the strength and depth of the DCM. The integrated chlorophyll is higher at the Alboran Sea with values ranging at stations P2 and P4 between 30 and 60 mg/m^2 (Tables 2—5). These values are even higher at the

Table 3 SPRING. Mixed layer depth (MLD), nutricline depth, integrated nitrogen (nitrate + nitrite), phosphate and silicate, integrated Dissolved Oxygen and chlorophyll, Deep Chlorophyll Maximum (DCM) concentration and depth and Secchi disk depth.

Spring	MLD (m)	Nut. Depth (m)	Int. N. (mmol/m^2)	Int. P. (mmol/m^2)	Int. Si. (mmol/m^2)	Int.DO. (L/m^2)	Int. Chl. (mg/m^2)	DCM (mg/m^3)	DCM depth (m)	Secchi (m)
P2	17	13	404	24	240	478	58	2.3	13	13
P3	22	19	344	22	216	386	43	1.5	21	
P4	25	13	514	42	236	468	48	1.2	36	18
M2	16	20	202	13	125	363	49	1.6	30	13
M3	18	27	299	18	231	393	29	1.2	32	
M4	18	30	291	15	120	477	57	1.4	33	16
V2	17	24	215	12	148	369	51	1.8	29	14
V3	17	20	341	20	218	399	46	1.7	21	
V4	19	33	319	21	158	486	53	1.2	42	16
S2	14	20	400	18	212	483	33	0.7	32	17
S4	20	28	359	18	196	480	47	1.3	38	17
CG2	21		10	8	51	352	14	0.4	55	15
CG4	19	60	162	19	172	504	25	0.6	55	23
CP2	16	50	86	7	94	399	28	0.7	44	20
CP3	19	78	78	9	104	544	13	0.4	53	
CP4	20	35	123	8	127	503	21	0.4	54	24
C20	15	34	152	7	135	473	27	0.5	46	19
C18	15	44	148	7	115	527	25	0.5	44	24
T2	30	45	57	5	35	409	21	0.4	45	22
T4	19					538	21	0.3	48	19
BNA2	53	67	94	2	111	526	23	0.4	50	23
BNA4	39	43	110	3	201	517	35	0.8	57	20
B1	17	51	55	2	82	383	21	0.6	64	26
B2	19	49	118	3	118	513	25	0.6	63	28
B3	20	61	123	3	134	533	18	0.4	57	28
MH2	33	48	151	6	185	541	23	0.6	40	24
MH4	24	33	151	6	175	527	28	0.5	53	25

M transect where 88 mg/m^2 are reached (Table 2). From Cape Gata transect to the north (CG, CP, C, B and MH transects) the minimum integrated values are observed, ranging along the seasonal cycle between 10 and 35 mg/m^2 (CG2 in Fig. 10), or even between 12 and 25 mg/m^2 in station B3 (Tables 2—5 and Fig. 11 for similar values at the B1 and B2 stations). Nutrient concentrations resemble the chlorophyll gradient with nitrate + nitrite integrated values ranging from 300 to 450 mmol/m^2 in P transect (Fig. 9) and similar values at the other Alboran stations from transect P to S, and then a clear decrease from CG transect (Fig. 10) to CP, C, B and MH transects where integrated nitrogen rarely exceeds 150 mmol/m^2. Integrated phosphate concentrations can reach values as high as 42 mmol/m^2 in the Alboran Sea, from Cape Pino (P, Fig. 9) to Sacratif (S). CG section shows integrated phosphate concentrations ranging between 4 and 19 mmol/m^2 (Fig. 10) and even lower values at sections CP, C, B (Fig. 11) and MH where concentrations are around 5 mmol/m^2. Nitrate + nitrite integrated concentrations in the northern transects BNA and MH are slightly higher than those from Cape Gata to the Balearic channels (transects C and B) with values reaching 247 mmol/m^2 at MH4 station and 184 mmol/m^2 in BNA4. On the contrary, integrated phosphates remain at very low values around 5 mmol/m^2 in the transects T, BNA and MH.

Secchi disk depth is maximum in summer when the integrated chlorophyll is lower, the nutricline is deeper and the MLD is shallower. The minimum Secchi disk depths are found in the P transect where the chlorophyll concentrations are highest (around 15 m). There are no significant differences between winter and summer values coinciding with the lack of a clear seasonal pattern for chlorophyll and nutrient concentrations. The summer maximum Secchi disk depth increases at section M (20 m) and V4 (25 m). S and CG transects show minimum values around 15 in winter and maximum values close to 25 m in summer. Similar values are observed in C, T and BNA transects. The clearest waters are found in CP4 where the summer Secchi disk depth reaches 30 m, and in the B and MH transects, with summer values higher than 30 m (Table S2).

3.4. Redfield ratios

For the calculation of the N:Si:P ratios, the RADMED stations were grouped into three different areas: Alboran (P, M, V, S and CG transects), peninsular eastern coast (CP, C, T and BNA transects) and Balearic Islands (B and MH transects). Nitrogen (Nitrate + nitrite), phosphate and silicate concentrations were also divided into two layers. The upper one extended from the surface to 75 m depth, representing the AW flowing in the upper layer of the Mediterranean Sea. The lower layer extended from 100 m to the bottom and represents waters with a higher percentage of Mediterranean water masses. N *versus* P data are presented in Figs. 12—14 for the three areas and the two layers considered. Following Pujo-Pay et al. (2011), the Redfield

Table 4 SUMMER. Mixed layer depth (MLD), nutricline depth, integrated nitrogen (nitrate + nitrite), phosphate and silicate, integrated Dissolved Oxygen and chlorophyll, Deep Chlorophyll Maximum (DCM) concentration and depth and Secchi disk depth.

Summer	MLD (m)	Nut. Depth (m)	Int. N. ($mmol/m^2$)	Int. P. ($mmol/m^2$)	Int. Si. ($mmol/m^2$)	Int.DO. (L/m^2)	Int. Chl. (mg/m^2)	DCM (mg/m^3)	DCM depth (m)	Secchi (m)
P2	13	29	351	21	257	471	57	1.5	24	15
P3	14	16	392	23	266	364	42	1.8	14	
P4	11	23	322	19	200	471	29	0.8	13	19
M2	14	32	180	13	129	352	38	1.4	29	17
M3	13	32	288	19	195	390	28	1.0	30	
M4	12	34	314	18	210	457	65	2.0	21	20
V2	14	30	173	11	129	368	35	1.0	38	20
V3	14	35	272	16	199	394	23	0.9	34	
V4	12	40	279	22	187	461	42	1.1	31	25
S2	13	35	216	9	155	473	31	0.8	50	26
S4	11	45	233	6	148	470	21	0.4	50	27
CG2	17	35	98	5	86	356	21	0.6	60	24
CG4	13	48	166	6	116	491	24	0.5	49	25
CP2	16	63	38	3	74	373	13	0.3	63	25
CP3	16	68	131	9	124	516	23	1.1	53	
CP4	14	63	87	4	88	458	19	0.4	63	30
C20	15	63	71	3	116	438	15	0.4	75	21
C18	17	73	91	5	100	506	21	0.4	67	24
T2	17	65	38	7	58	385	16	0.7	75	22
T4	13	65	65	3	107	479	18	0.4	75	26
BNA2	13	80	55	4	82	514	20	0.4	67	25
BNA4	15	63	137	9	133	512	19	0.4	50	23
B1	21	70	23	4	59	353	15	0.5	63	31
B2	20	64	99	3	106	459	15	0.3	68	33
B3	20	60	147	7	130	493	13	0.3	58	32
MH2	14	78	69	3	101	526	15	0.4	88	29
MH4	17	68	109	6	137	513	19	0.4	75	32

ratios were calculated using two different methods. For the first one, the Redfield ratio was estimated as the slope of the regression line fitted to the N:P and Si:P data (see Figs. 12—14). For the second one, mean N, Si and P concentrations were calculated for each area and layer and then the corresponding ratio was calculated. In both cases, 95% confidence intervals were estimated using a *t*-student distribution for the slope of the regression line and for the mean nutrient concentrations (see for instance Zar, 1984). Errors for the ratios were derived from the mean concentration confidence intervals using the error propagation formulae for the quotient. The Redfield ratios estimated using both methods, including the confidence limits at the 95% confidence level have been included in Figs. 12—14. Upper numbers correspond to the slope of the linear fit and the lower numbers correspond to the ratio of the mean N and P concentrations.

Different results were obtained depending on the calculation method used. Nevertheless, if the 95% confidence intervals are considered, both results (regression and ratio between mean concentrations) overlap. For the upper layer of the Alboran Sea, N:P ratios are higher than the theoretical 16 value when the regression line is considered while the values are 16 or lower if the mean N and P concentrations are divided. Notice that if the lower limit is considered, the regression line also would yield ratios close to 16. Si:P ratios (not shown) for the upper Alboran Sea were lower than the 15 theoretical value in all the cases. More contradictory results were obtained for the lower layer (100 m—bottom). If the slope of the regression line was considered, values ranging from 10 to 20 were obtained, depending on the season. On the contrary, if mean concentrations were divided, the N:P ratio ranged from 17 (autumn) to 24 (summer). Considering the uncertainty in the calculations, Si:P ratios varied along the seasonal cycle around the 15 value.

For the peninsular eastern coast, the upper layer N:P values showed a very large dispersion with some unrealistic results such as the 2 ± 5 value for the summer season. N:P ratios based on mean concentrations oscillate between 23 ± 9 for winter and 11 ± 7 for summer. Notice that the lower limit for the winter interval would be 14. This ratio is close to 16 if an average value is calculated for the whole year. Once again very low values are obtained for the lower layer if the first method is applied (see Fig. 13), while values ranging from 19 to 22 are obtained for the second one. Similar results are observed when the Si:P ratio is analyzed, with very low values for the regression line in both the upper and lower layer and higher values for the ratio between mean concentrations. For the latter case, the Si:P ratio is above 15 for most of the cases.

3.5. Decadal changes

Chlorophyll and nutrient time series in the Malaga Bay and Cape Palos regions were initiated under the umbrella of previous projects: ECOMALAGA and ECOMURCIA in

Table 5 AUTUMN. Mixed layer depth (MLD), nutricline depth, integrated nitrogen (nitrate + nitrite), phosphate and silicate, integrated Dissolved Oxygen and chlorophyll, Deep Chlorophyll Maximum (DCM) concentration and depth and Secchi disk depth.

Autumn	MLD (m)	Nut. Depth (m)	Int. N. (mmol/m^2)	Int. P. (mmol/m^2)	Int. Si. (mmol/m^2)	Int.DO. (L/m^2)	Int. Chl. (mg/m^2)	DCM (mg/m^3)	DCM depth (m)	Secchi (m)
P2	19	23	401	24	262	483	47	1.5	16	16
P3	16	11	433	27	289	379	23	0.9	10	
P4	28	18	458	30	317	499	32	0.8	15	18
M2	17	27	216	15	157	367	41	1.1	24	17
M3	20	23	376	22	252	377	28	1.0	24	
M4	18	30	375	21	238	486	33	0.9	18	18
V2	17	30	197	14	144	358	31	1.0	18	18
V3	20	31	326	21	203	389	26	1.0	18	
V4	18	24	417	26	265	490	58	2.3	23	18
S2	30	26	418	21	323	494	23	0.8	22	20
S4	28	23	414	22	256	504	44	1.6	25	21
CG2	29	35	138	8	105	386	32	0.8	38	21
CG4	28	33	269	14	174	524	27	0.6	40	23
CP2	38	18	147	9	99	383	25	0.7	22	20
CP3	39	55	175	8	136	508	17	0.5	30	
CP4	33	36	193	12	127	484	31	0.9	30	24
C20	54	43	86	5	153	417	19	0.3	44	20
C18	38	88	76	3	111	548	21	0.3	56	22
T2	34	60	37	4	87	412	10	0.1	35	24
T4	35	50	175	8	185	528	14	0.3	33	22
BNA2	51	65	103	4	127	559	17	0.3	27	17
BNA4	42	69	60	3	117	561	16	0.2	16	21
B1	39	63	25	2	64	353	14	0.3	50	26
B2	42	61	72	4	99	520	15	0.3	50	27
B3	41	62	85	3	87	540	17	0.3	50	27
MH2	42					506	15	0.3	50	23
MH4	40	100	35	4	79	514	14	0.2	28	26

1992 and 1996 respectively. Beside the existence of some gaps caused by bad weather conditions, instrument failures, and vessel availability, data obtained from these projects and the present RADMED program provide 20 year-long time series for chlorophyll-*a*, nutrient and DO concentrations. Stations P3, M3 and V3 are the longest and best sampled time series in the Malaga Bay area. CP3 is the best-sampled station at Cape Palos transect. Once the seasonal cycle was subtracted for each data point, residuals or deviations from the seasonal cycle were obtained. Residuals time series for P3, M3, V3 and CP3 are presented in Fig. 15. For each station, the left plot shows the nutricline depth (black line) and the integrated nitrogen (light brown) and integrated phosphate concentrations (dark brown). The right plot shows the DCM depth (black line), the chlorophyll concentration at the DCM (purple) and the integrated chlorophyll concentration (dark green).

For the P3 case, the only variables which showed a significant trend (at the 0.05 significance level) were the integrated chlorophyll, which increased along the considered period at a rate of 1.3 ± 1.1 mg m^{-2}/yr and the integrated DO (not shown) which increased at a rate of 3.0 ± 1.6 lm^{-2}/yr. Similarly, integrated chlorophyll and DO also increased in a significant way at M3 station with trends of 1.3 ± 0.8 mg m^{-2}/yr and 1.9 ± 1.7 lm^{-2}/yr. This chlorophyll and DO increase at M3 was accompanied by nitrogen and phosphate negative trends of -5.4 ± 5.3 and -0.5 ± 0.3 mmol m^{-2}/yr respectively. Once again integrated chlorophyll and DO showed positive trends for V3 (1.4 mg m^{-2}/yr and 2.1 ± 1.5 lm^{-2}/yr), while nutrient trends were not significant. No clear results were obtained for the MLD trends which were not significant in most of the cases and showed positive and negative values. Finally, trends in CP3 station were not significant with the only exception of the integrated DO which decreased at a rate of -2.1 ± 1.8 lm^{-2}/yr.

4. Discussion and conclusions

RADMED stations cover an area with important oceanographic differences. The westernmost stations in the Alboran Sea are close to the Strait of Gibraltar (mainly P and M transects) and therefore are subject to the direct influence of the AW. The northernmost stations, (T and BNA transects) receive AW severely modified after recirculation along the whole Western Mediterranean (northern current). The AW continues its pathway southward and partially flows along the Ibiza Channel, while another branch of this current turns to the north of the Balearic Islands feeding the Balearic current (see Fig. 1 and Pinot et al., 1995; Pinot and Ganachaud, 1999). MH transect would be affected by this current while the C20 and C18 stations would be under the influence of the southward extension of the northern current. According to this simplified circulation scheme, the AW reaching the MH and C

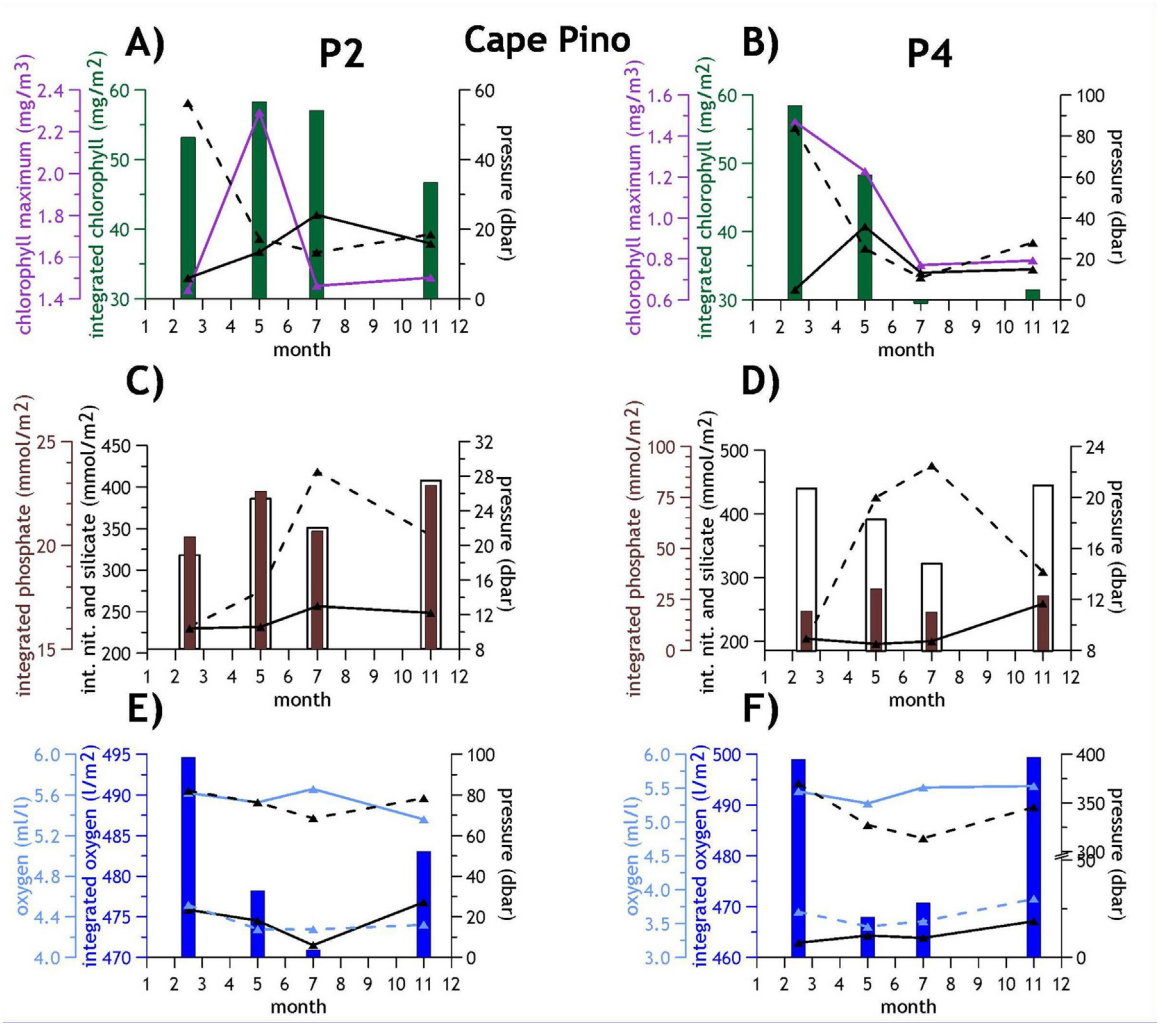

Fig. 9 Stations P2 and P4, Cape Pino transect. (A) and (B) Mixed layer depth (MLD, black dashed line), DCM depth (black solid line), chlorophyll-*a* maximum concentration (purple), integrated chlorophyll-*a* (dark green). (C) and (D) integrated phosphate (dark brown bars), integrated nitrate (white bars), integrated silicate (continuous black line) and nutricline depth (dashed black line). (E) and (F) maximum Dissolved Oxygen concentration (light blue solid line) and depth (black solid line) minimum Dissolved Oxygen concentration (light blue dashed line) and depth (black dashed line) and integrated Dissolved Oxygen (dark blue bar). (For interpretation of the references to colour in this figure legend, the reader is referred to the web version of this article.)

transects would be modified after a residence time within the WMED longer than the one corresponding to the T and BNA stations. Nevertheless, the Balearic Channels are a transition zone between the AW recently advected into the Mediterranean Sea through the Strait of Gibraltar and the AW to the north, modified by evaporation and mixing with Mediterranean waters. According to Millot (1999) and Pinot et al. (1995, 1999), AW trapped in anticyclonic gyres would detach from the Algerian current and cross northward the Balearic Channels. These traits of the AW circulation within the WMED are reflected in the θS distributions presented in Fig. 2. There is a clear salinity gradient from Cape Pino stations to BNA transect with the Balearic Islands showing intermediate θS properties between the Alboran Sea and the Catalan Sea stations. Another interesting feature observed in the average θS diagrams is the low potential temperature (<13°C) observed in winter in BNA stations. This is an indication of WIW formation and therefore intermediate convection that could account for the mixing of the upper 200–300 m in the Catalan continental shelf and slope and the winter nutrient injection to the photic layer. These cold waters above the LIW are also observed in spring, summer and autumn in BNA and MH transects, but in this case, this would only reflect the arrival of WIW formed to the north (Gulf of Lions) during the previous winter. θS values for all the stations lie on the mixing line between the NACW and the LIW (200–600 m), characterized by a salinity maximum, and the WMDW from 600 m to the bottom in the deep stations.

The distribution of water masses and their circulation have a clear influence on the nutrient and DO concentrations along the Spanish Mediterranean waters. First, the highest nitrate concentrations are observed in the westernmost Alboran Sea decreasing eastwards to Cape Gata during all the seasons. Low nitrate concentrations (compared with the

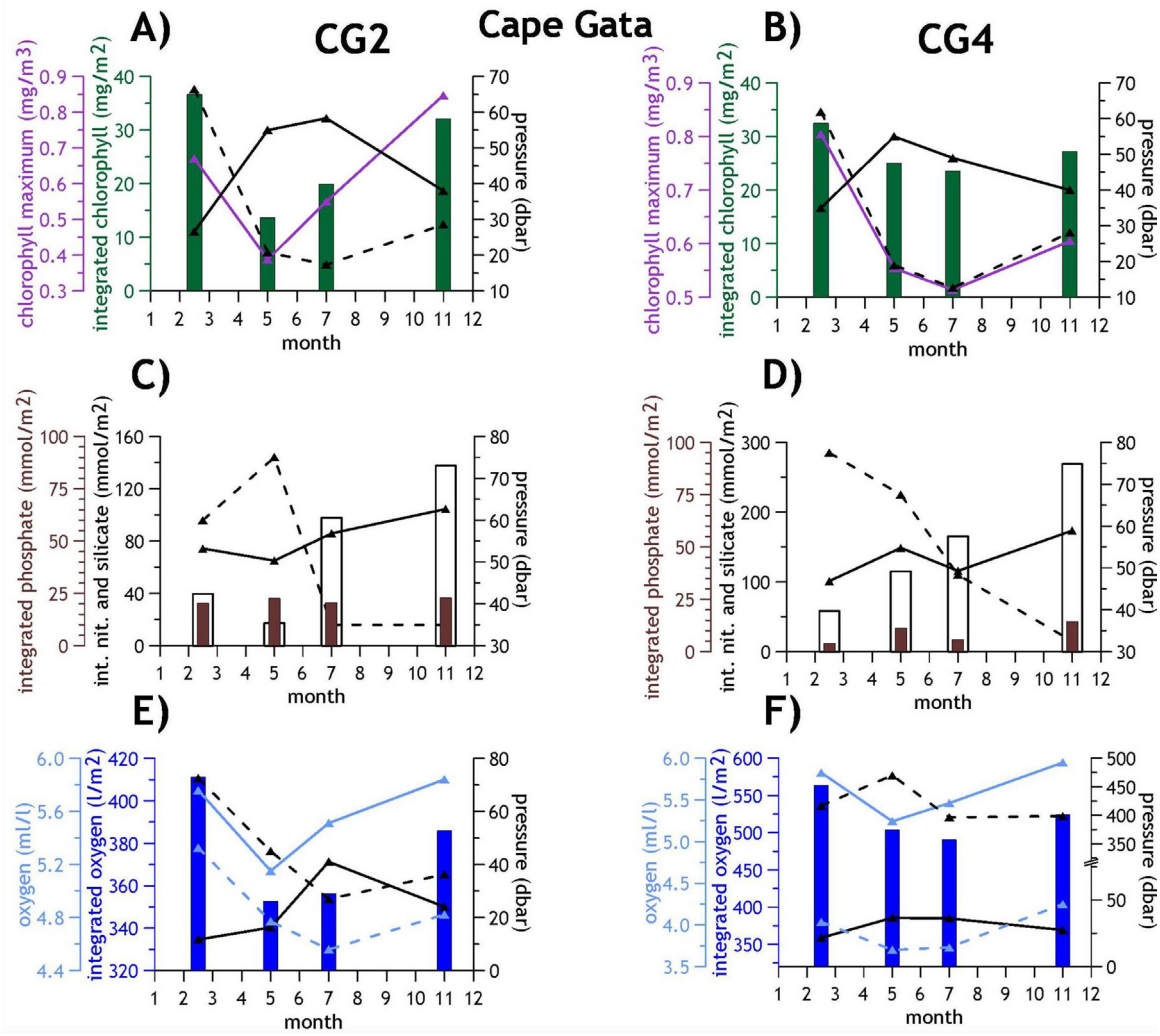

Fig. 10 The same as in Fig. 9, but for CG2 and CG4 stations in Cape Gata transect.

Alboran Sea) are observed for all the stations to the north of Cape Gata (Tables 2—5). This difference is even clearer for the phosphate concentrations which can reach 42 mmol/m^2 in spring at P4 station, while they are around 2 or 3 mmol/m^2 in BNA and B transects. Maximum surface nitrate concentrations are frequently found in winter or spring (see Table S1), although some stations present surface maxima in autumn (CG2, CP2, B2, B3). In most of the cases, the nutricline is at its deepest level in summer (Figs. 9—11) when the MLD is at its shallowest position. Nitrate and phosphate increase with the depth reaching a maximum between 200 and 500 m, which is clearly observable in those stations deeper than 500 m (see for instance Figs. 4 and 6). These nutrient maxima are associated to the LIW. This water mass is formed in the Eastern Mediterranean and flows into the WMED through the Strait of Sicily. This water mass describes a cyclonic circuit within the WMED similar to that followed by the AW (see for instance Millot, 1999). Remineralization of organic matter sunk during the LIW formation and from the photic layer above is responsible for the nutrient increase in the LIW. The same reason would explain the DO minimum at the same depth level (Figs. 4 and 6). LIW flows along the northern part of the WMED following the northern current, then flows southward through the Ibiza Channel and finally turns to the west in the Alboran Sea towards the Strait of Gibraltar. For this reason, the P, M and V transects are the last ones to receive the LIW. Organic matter oxidation during this long time could be responsible for the lower values of the DO minimum which is between 3.6 ml/l and 3.9 ml/l in the Alboran Sea and above 4 ml/l for those stations to the east and north of Cape Gata. Another explanation for the lower values of the DO minimum in the Alboran Sea would be the DO extra-minimum described by Minas et al. (1991). Notice that P3, P4, V3 and S2 stations show DO concentrations ranging between 3.6 and 3.8 ml/l at 300 m. According to Minas et al. (1991), the high primary production at the eastern side of the Strait of Gibraltar and the Northwestern Alboran Sea, and the oxidation of the organic matter exported below the photic layer would be responsible for the existence of this DO extra minimum lower than the one associated to the LIW.

The high primary production at the Northwestern Alboran Sea has been related to the enrichment of surface waters at the Strait of Gibraltar as a consequence of internal tide mixing and the upward movement of the AW flowing through Gibraltar (Echevarría et al., 2002; Gómez et al., 2000; Gómez, 2003; Huertas et al., 2012; Reul et al., 2005). The

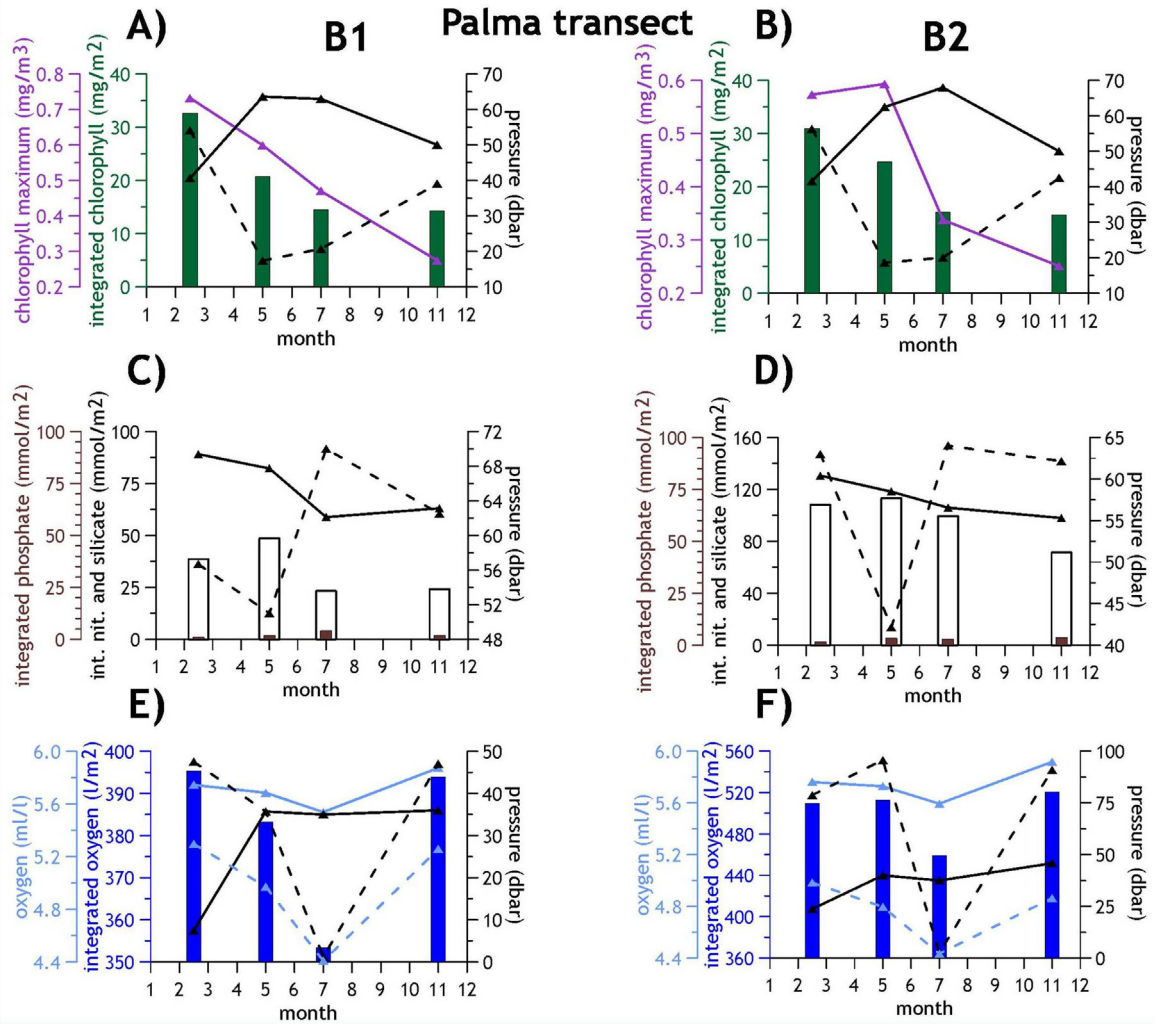

Fig. 11 The same as in Figs. 9 and 10, but for B1 and B2 stations in Mallorca transect.

high chlorophyll concentrations observed in the northern sector of the Alboran Sea and mainly along the Atlantic Jet which surrounds the Western Alboran gyre would be partially produced by the phytoplankton uptake of nutrients upwelled at the northeastern side of Gibraltar (Ruiz et al., 2001). On the other hand, cyclonic circulation cells between Punta Europa (Strait of Gibraltar) and Cape Pino, and in front of Malaga Bay would also be responsible for high primary production rates (Reul et al., 2005; Sarhan et al.,2000). These circulation patterns would be reflected in the high surface and integrated chlorophyll concentrations in the P, M and V transects. Notice that integrated chlorophyll concentrations do not show a clear seasonal pattern at these stations as high values are observed during the stratified season: summer and autumn (65 mg/m^2 in summer at M4 station and 47 mg/m^2 at P2 in autumn). Beside this, the DCM (or subsurface chlorophyll maximum) is always at the upper 20 m of the water column (Tables 2—5). All these facts suggest the high influence of permanent upwelling mechanisms operating in the Western Alboran Sea throughout the whole year.

Tables 2—5 show clearly the SW-NE trophic gradient in the RADMED area. The chlorophyll concentration at the DCM decreases clearly from the top of the table (Alboran Sea) to the bottom (Balearic stations). At the same time, the depth of the DCM increases in the same direction. Nevertheless, high nutrient and chlorophyll concentrations are observed in winter in BNA4 and MH4 stations. These results are coincident with the existence of very low winter temperatures which could indicate the influence of strong winter mixing and intermediate convection on the fertilization of these areas.

Redfield ratios have been calculated for three geographical areas: the Alboran Sea, the peninsular part of the Eastern Spanish coast and the Balearic Islands. Two different approaches were used. For the first one, all nitrate + nitrite values and all the phosphate values from the upper layer (0—75 m) were chosen and the same was done for the lower layer (100 m—bottom). A regression line was fitted to the nitrogen-phosphate data and the slope was considered as the N:P Redfield ratio. The same procedure was followed for the Si:P ratio. The results from this method seem to be very dispersed with confidence intervals exceeding the ratio value. The second method consisted in the estimation of the nitrogen (nitrate + nitrite), phosphate and silicate mean concentrations for each layer and then the calculation of the corresponding ratios: N:P and Si:P. This second approach seemed to yield more coherent results in the case of the Alboran Sea and the peninsular eastern coast. For the Alboran

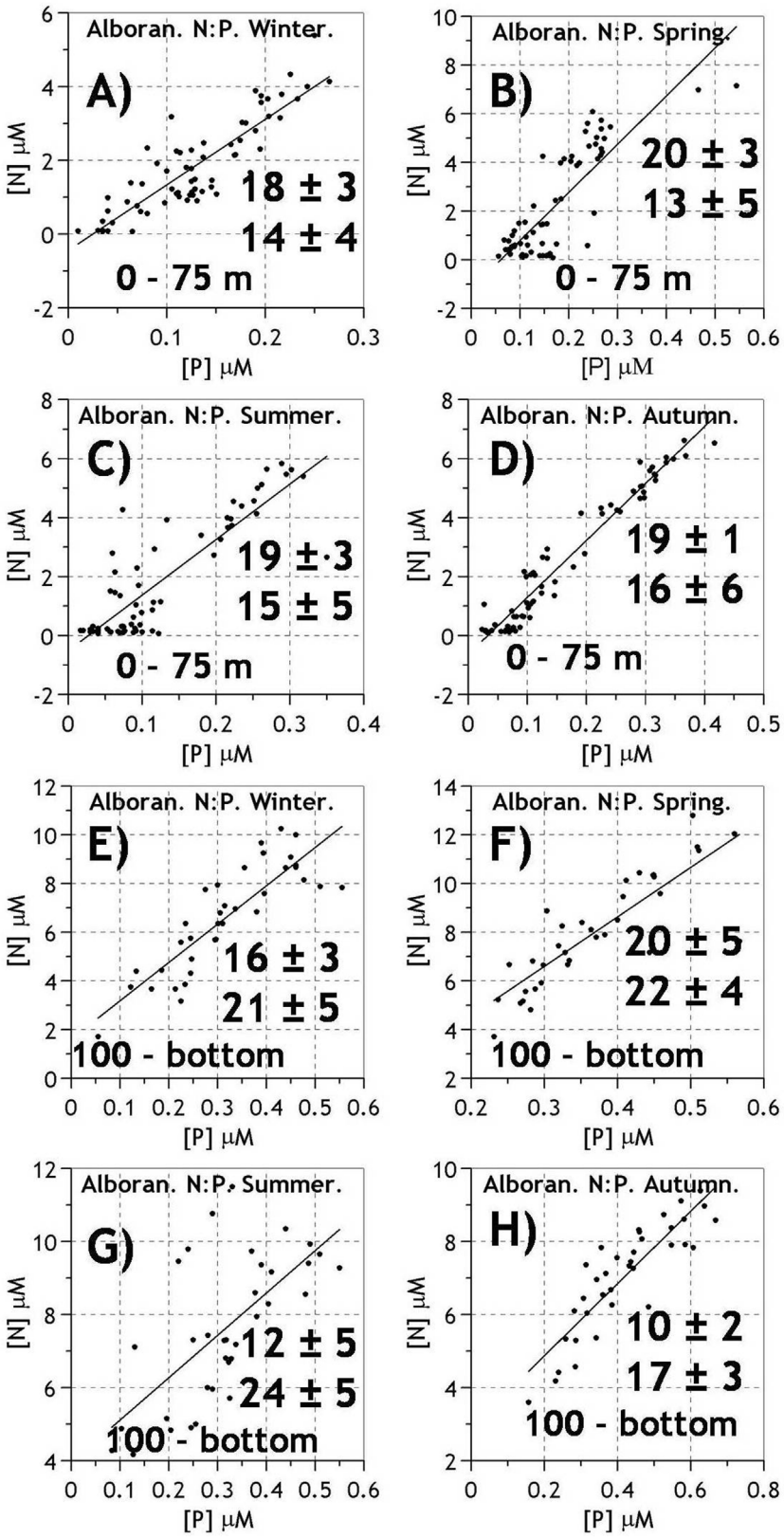

Fig. 12 Redfield N:P ratios for the 0—75 m layer for the Alboran Sea. Fig. 12A is for winter, 12B for spring, 12C for summer and 12D for autumn. Figs. 12E, F, G and H are the same for the 100 m-bottom layer.

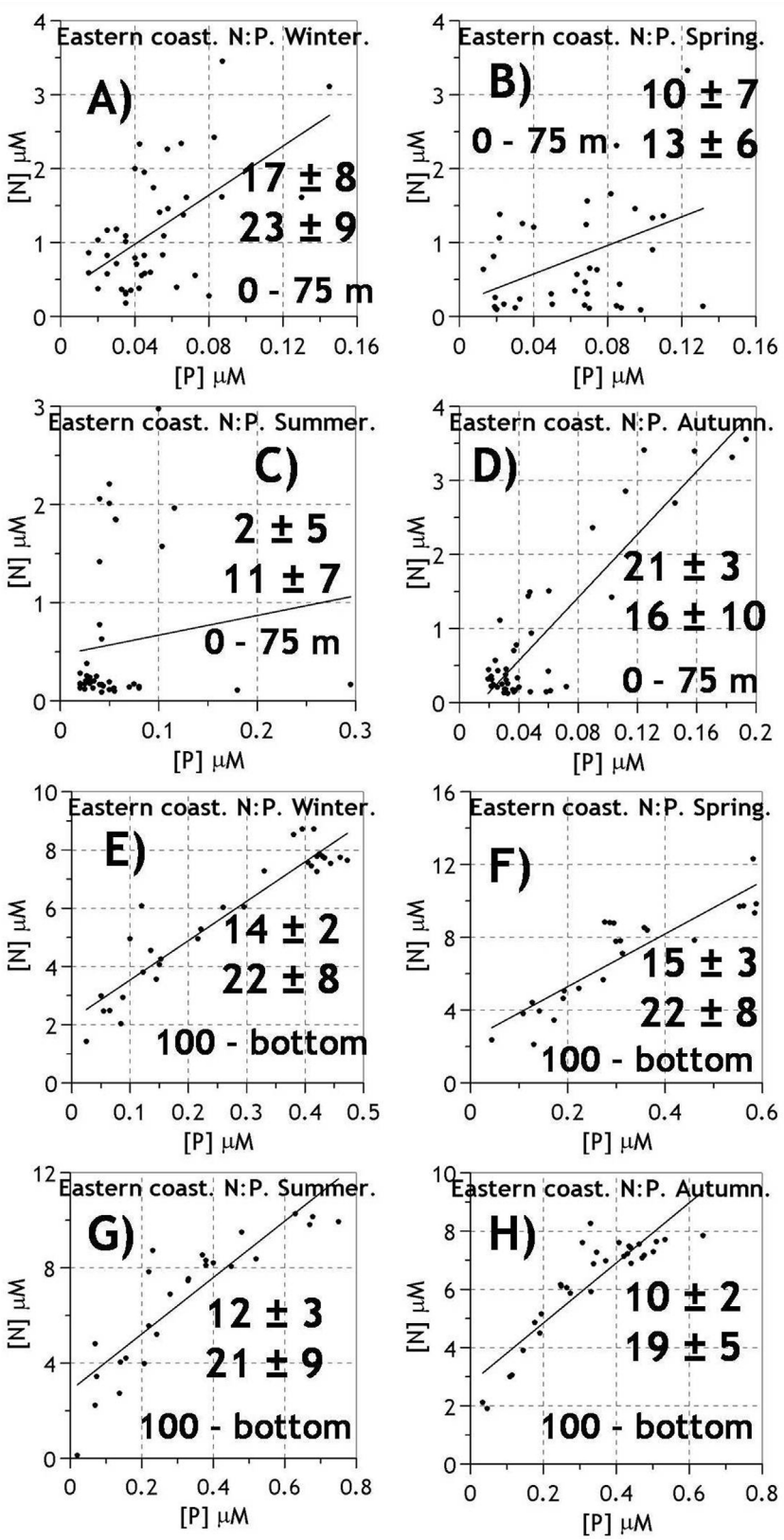

Fig. 13 The same as in Fig. 12, but for the peninsular eastern Spanish Mediterranean.

Sea, N:P ratios for the upper layer changed with the season between 13 and 16 with an annual mean value of 15. For the deep layer the values ranged between 17 and 24 with an annual mean value of 21. Very similar results were obtained for the peninsular eastern coast with N:P ratios of 16 and 22 for the upper and lower layers respectively. The Redfield ratios estimated for the Balearic Islands were very dispersed, very likely as a consequence of the data scarcity. Taking into

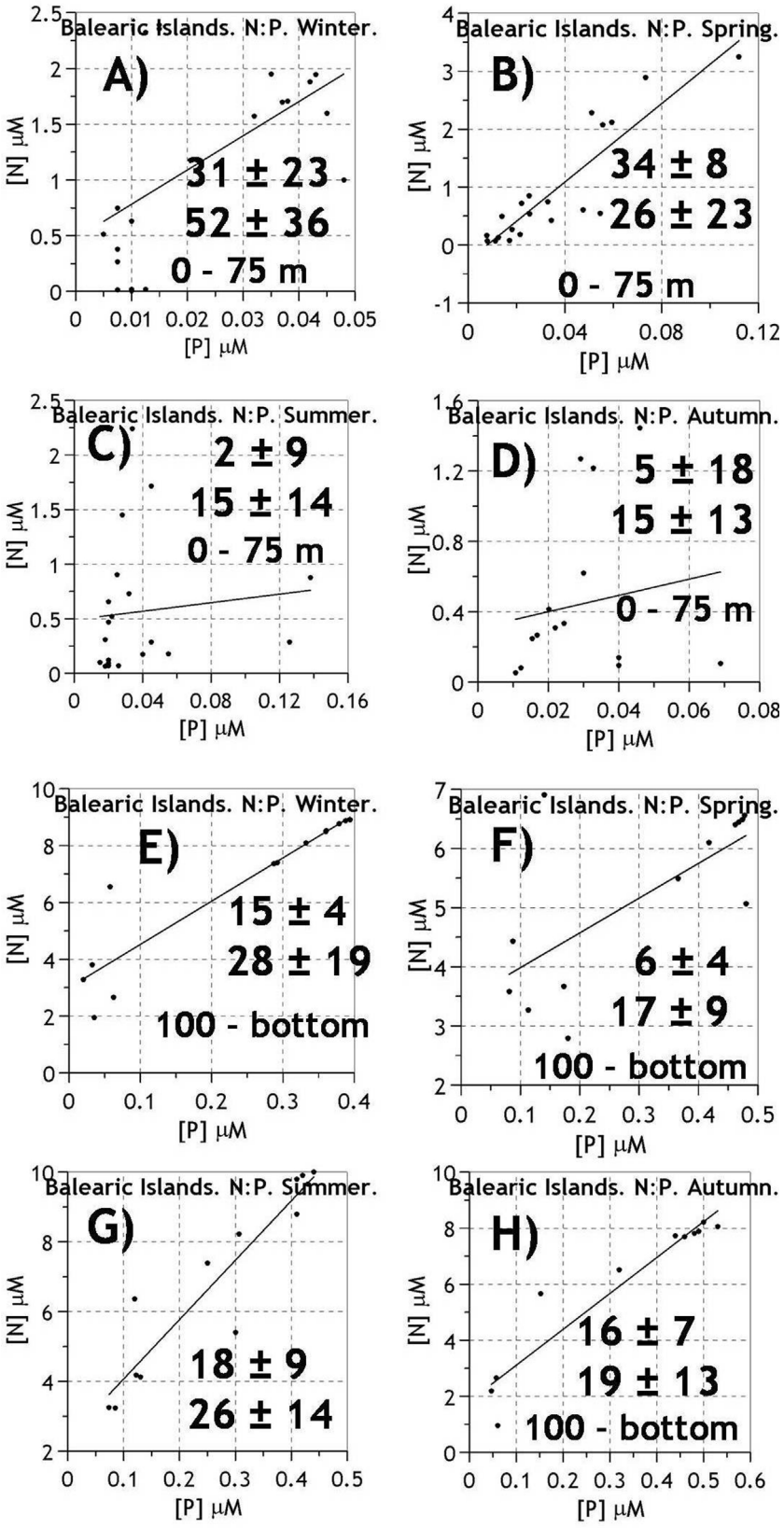

Fig. 14 The same as in Figs. 12 and 13, but for the Balearic Islands.

account the Alboran Sea and eastern coast results, it can be established that the upper layer follows the theoretical ratio 16, while the ratio for the deep layer clearly exceeds this value as already reported in previous works. This result would suggest that there is no phosphorus limitation for the AW within the westernmost sector of the Mediterranean Sea,

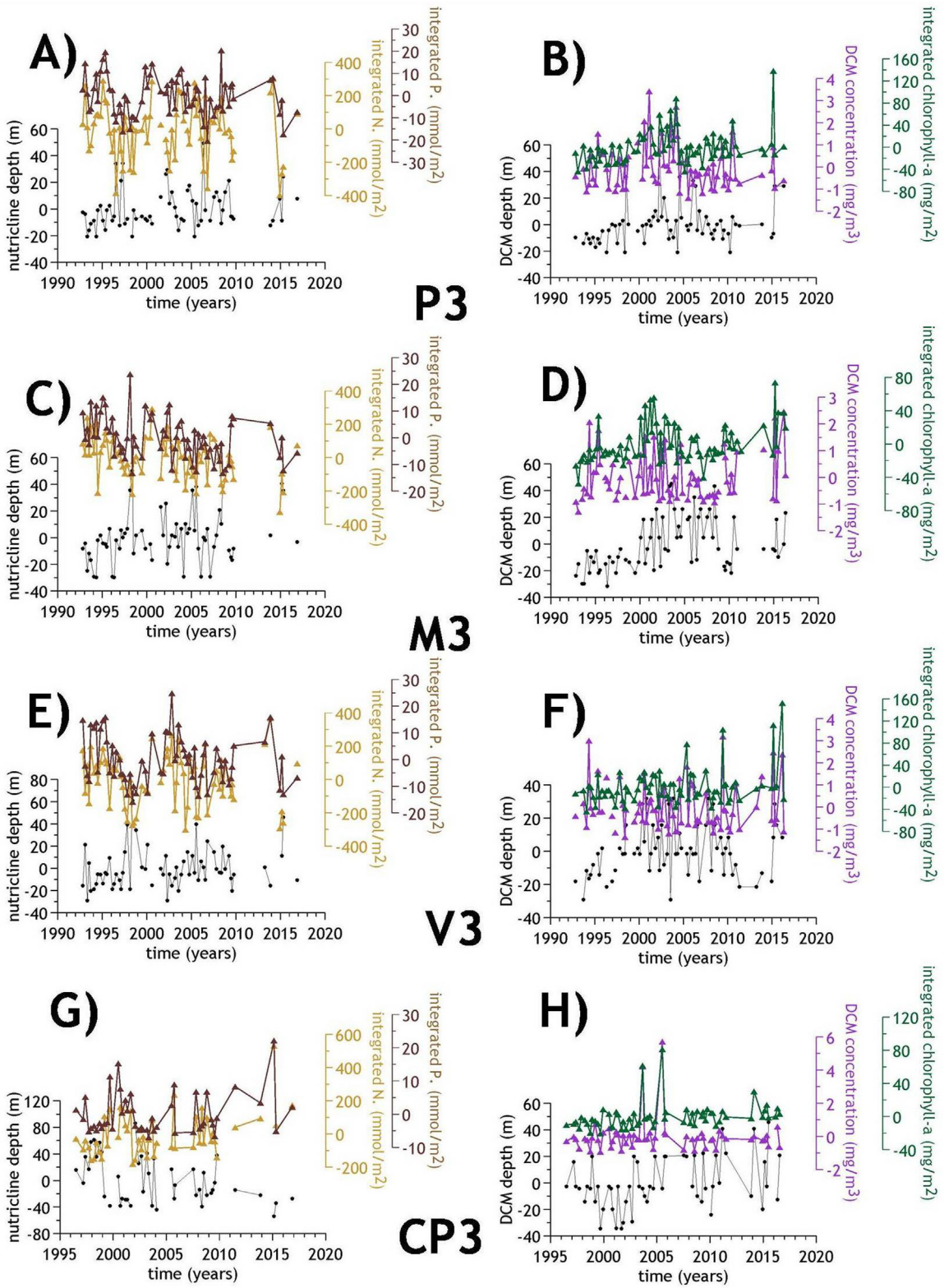

Fig. 15 Figures A, B show the residuals time series (deviations from the seasonal cycle) for the P3 station. Fig. 15A shows the nutricline depth (black line), the nitrate concentration integrated to the 100 m depth (light brown) and the integrated phosphate concentrations (dark brown). Fig. 15 B shows the residuals for the DCM (black line), the chlorophyll concentration at the DCM (purple) and the integrated chlorophyll (dark green). Fig. 15 C, D are the same for the M3 station, Fig. 15 E, F are the same for V3 station and Fig. 15 G, H for CP3 station. (For interpretation of the references to colour in this figure legend, the reader is referred to the web version of this article.)

while this limitation exists for the eastern basin (Thingstad et al., 2005) where LIW is formed. Notice that this water mass occupies the 150—600 m layer within the WMED and is also a main contributor to the WMDW formation.

Finally, the lengths of the present time series do not allow us to estimate long-term changes. Nevertheless, time series at the Malaga Bay area (P, M and V transects) and the Cape Palos area (CP) are suitable for the estimation of the decadal variability from the beginning of the 1990s to 2015. Linear trends for integrated nutrient concentrations, integrated chlorophyll-*a* and DO, nutricline depth and MLD, DCM chlorophyll concentration and DCM depth were estimated for these transects. Most of the trends obtained were not statistically significant at the 0.05 significance level. One of the threats on the Mediterranean Sea and the global ocean is the increase of the water column stratification as a consequence of the upper layer warming. This warming and stratification would produce the decrease of the DO solubility, lower ventilation rates for the intermediate and deep layers and the decrease of the nutrient injection into the photic layer. More stratified waters would require a higher kinetic energy to be mixed during autumn, winter and early spring. Therefore the MLD could be considered as a good indicator of these processes. Time series from 1992 to 2015 in the Malaga Bay area and from 1996 to 2015 in the Cape Palos transect did not show significant changes in the MLD. The only significant trends were obtained in M2 station with a positive trend of 0.28 ± 0.26 m/yr (deepening of the MLD) and at V3, with a negative trend of -0.29 ± 0.26 m/yr. The results were not significant for the other stations and therefore it cannot be concluded the existence of changes in the MLD in these two regions. The only significant trends were those obtained for the integrated chlorophyll and DO in the P3, M3 and V3 stations. Both variables increased for the 1992—2015 period indicating a possible increase in the primary production in the Western Alboran Sea.

In summary, the RADMED monitoring program has allowed us to establish a clear trophic gradient from the southwest to the northeast in the Spanish Mediterranean waters as well as the main traits of the nutrient, DO and chlorophyll distributions. Nitrate concentrations at the upper layers of the water column reach maximum values during winter mixing. Nevertheless some exceptions are observed in S and CG transects (Eastern Alboran Sea) and in B2 and B3 stations in Mallorca transect. In these cases, the surface nitrate maximum is advanced to autumn when stormy conditions usually begin. Notice that the autumn nitrate estimations are based on 4 autumn cruises for the case of S and CG transects and 7 cruises for the case of B transect. Phosphate concentrations at the upper layer seem to be more homogeneous along the year without a clear seasonal cycle. The nitrate surface injection decreases from the southwest to the northeast. The only exceptions are BNA4 station and the MH transect with surface winter nitrate concentrations close to or higher than 1 μM. Notice that these stations are located in areas of intermediate winter convection (Vargas-Yáñez et al., 2012). The intensity of the DCM decreases and its depth increases from the Alboran Sea to the northeast. The DCM is accompanied by a DO maximum at the same depth or above it and a nitrite maximum which has been attributed to incomplete assimilatory reduction of nitrate by phytoplankton. Redfield ratios seem to indicate phosphorus limitation for the intermediate and deep layers, but not for the AW occupying the 0—75 m layer of the water column. The longest time series are those corresponding to P, M and V transects in the Western Alboran Sea and CP to the south of Cape Palos. The only significant trends observed show an increase of the chlorophyll and DO content in the P, M and V transects. Nevertheless, the length of these time series precludes us from considering that these decadal changes could be considered as the long-term trend.

Finally, some of the seasonal estimations presented in the present work are based on more than 15 or 20 data per season and therefore mean values and variability ranges could be provided (see Table S1). Mean values and standard deviations obtained in this way could be used as a reference for future works or operational services providing reference values and ranges of variability. On the other hand, transects recently included in the monitoring program and the frequent difficulties such as bad weather conditions, instrument failures and vessel availability do not allow us to present robust statistics in some cases. These estimations, although based on very scarce data are presented for the completeness of the work and for showing the importance of such monitoring programs for base line setting and trend detection in the context of global change scenario.

Acknowledgements

The RADMED monitoring program is funded by the Instituto Español de Oceanografìa, and has been partially funded by the DESMMON project (PN I+D+I CTM2008-05695-C02-01), the PERSEUS project (FP7-287600), the IRIS-SES project (DG ENV GA-07.0335/2013/659540/SUB/C2.), the ActionMed project (DG-ENVGA-11.0661/2015/12631/SUB/ENVC.2) ATHAPOC project (PN I+D+I CTM2014-54374-R).

Appendix A. Supplementary data

Supplementary material related to this article can be found, in the online version, at https://doi.org/10.1016/j.oceano.2018.08.003.

References

Bethoux, J.P., Morin, P., Chaumery, C., Connan, O., Gentili, B., Ruiz-Pino, D., 1998. Nutrients in the Mediterranean Sea, mass balance and statistical analysis of concentrations with respect to environmental change. Mar. Chem. 63 (1—2), 155—169, http://dx.doi.org/10.1016/S0304-4203(98)00059-0.

Bethoux, J.P., Morin, P., Ruiz-Pino, D.P., 2002. Temporal trends in nutrient ratios: chemical evidence of Mediterranean ecosystem changes driven by human activity. Deep-Sea Res. Pt. II 49 (11), 2007—2015, http://dx.doi.org/10.1016/S0967-0645(02)00024-3.

Calvo, E., Simó, R., Coma, R., Ribes, M., Pacual, J., Sabatés, A., Gili, J.M., Pelejero, C., 2011. Effects of climate change on Mediterranean marine ecosystems: the case of the Catalan Sea. Clim. Res. 50 (1), 1—26, http://dx.doi.org/10.3354/cr01040.

Coll, M., Piroddi, C., Albouy, C., Rais Lasram, F.B., Cheung, W.W.L., Christensen, V., Karpouzi, V.S., Guilhaumon, F., Mouillot, D., Paleczny, M., Palomeras, M.L., Steenbeek, J., Trujillo, P., Watson, R., Pauly, D., 2011. The Mediterranean Sea under siege: spatial overlap between marine biodiversity, cumulative threats and

marine reserves. Glob. Ecol. Biogeogr. 21 (4), 465—480, http://dx.doi.org/10.1111/j.1466-8238.2011.00697.x.

De Boyer Montégut, C., Madec, G., Fischer, A.S., Lazar, A., Iudicone, D., 2004. Mixed layer depth over the global ocean: an examination of profile data and a profile-based climatology. J. Geophys. Res. 109 (C12), C12003, http://dx.doi.org/10.1029/2004JC002378.

D'Ortenzio, F., Ribera d'Alcala, M., 2009. On the trophic regimes of the Mediterranean Sea: a satellite analysis. Biogeosciences 6 (2), 139—148, http://dx.doi.org/10.5194/bg-6-139-2009.

Echevarría, F., García-Lafuente, J., Bruno, M., Gorsky, G., Goutx, M., Gonzalez, N., García, C.M., Gómez, F., Vargas, J.M., Picheral, M., Striby, L., Varela, M., Alondo, J.J., Reul, A., Cózar, A., Prieto, L., Sarhan, T., Plaza, F., Jiménez-Gómez, F., 2002. Physical—biological coupling in the Strait of Gibraltar. Deep-Sea Res. II 49, 4115—4130, http://dx.doi.org/10.1016/S0967-0645(02)00145-5.

Estrada, M., Latasa, M., Emelianov, M., Gutiérrez-Rodríguez, A., Fernández-Castro, B., Isern-Fontanet, J., Mouriño-Carballido, B., Salat, J., Vidal, M., 2014. Seasonal and mesoscale variability of primary production in the deep winter-mixing region of the NW Mediterranean. Deep-Sea Res. Pt. I 94, 45—61, http://dx.doi.org/10.1016/j.dsr.2014.08.003.

Estrada, M., 1996. Primary production in the northwestern Mediterranean. Sci. Mar. 60 (Suppl. 2), 55—64.

Garcia-Martinez, M.C., Vargas-Yañez, M., Moya, F., Zunino, P., Bautista, B., 2018. The effects of climate change and rivers damming in the Mediterranean Sea during the twentieth century. Int. J. Environ. Sci. Nat. Res. 8 (4), 555741, http://dx.doi.org/10.19080/IJESNR.2018.08.555741.

Gasol, J.M., Cardelús, C., Anxelu, X., Morán, G., Balagué, V., Forn, I., Marrasé, C., Massana, R., Pedrós-Alió, C., Montserrat Sala, M., Simó, R., Vaqué, D., Estrada, M., 2016. Seasonal patterns in phytoplankton photosynthetic parameters and primary production at a coastal NW Mediterranean site. Sci. Mar. 80 (S1), 63—77, http://dx.doi.org/10.3989/scimar.04480.06E.

Gómez, F., 2003. The role of the exchanges through the Strait of Gibraltar on the budgets of elements in the Western Mediterranean Sea: consequences of human-induced modifications. Mar. Pollut. Bull. 46 (6), 685—694, http://dx.doi.org/10.1016/S0025-326X(03)00123-1.

Gómez, F., González, N., Echevarría, F., García, C.M., 2000. Distribution and fluxes of dissolved nutrients in the Strait of Gibraltar and its relation to microphytoplankton biomass. Estuar. Coast. Shelf Sci. 51 (4), 439—449, http://dx.doi.org/10.1006/ecss.2000.0689.

Grasshof, K., Erhardt, M., Kremling, K., 1983. Methods of Seawater Analysis, 2nd edn. Verlag Chemie, Weinheim, 419 pp.

Holm-Hansen, O., Lorenzen, C.J., Holmes, R.W., Strickland, J.D., 1965. Fluorometric determination of chlorophyll. J. Mar. Sci. 30 (1), 3—15, http://dx.doi.org/10.1093/icesjms/30.1.3.

Huertas, I.E., Ríos, A.F., García-Lafuente, J., Navarro, G., Makaoui, A., Sánchez-Román, A., Rodríguez-Gálvez, S., Orbi, A., Ruiz, J., Pérez, F.F., 2012. Atlantic forcing of the Mediterranean oligotrophy. Global Biogeochem. Cycle 26 (2), GB2022, http://dx.doi.org/10.1029/2011GB004167.

Labasque, T., Chaumery, C., Aminot, A., Kergoat, G., 2004. Spectrophotometric Winkler determination of DO: re-examination of critical factors and reliability. Mar. Chem. 88 (1—2), 53—60, http://dx.doi.org/10.1016/j.marchem.2004.03.004.

Latasa, M., Gutiérrez-Rodríguez, A., Cabello, A.M., Scharek, R., 2016. Influence of light and nutrients on the vertical distribution of marine phytoplankton groups in the deep chlorophyll maximum. Sci. Mar. 80 (S1), 57—62, http://dx.doi.org/10.3989/scimar.04316.01A.

Latasa, M., Scharek, R., Vidal, M., Vila-Reixach, G., Gutiérrez-Rodríguez, A., Emelianov, M., Gasol, J.M., 2010. Preferences of phytoplankton groups for waters of different trophic status in the northwestern Mediterranean Sea. Mar. Ecol. Prog. Ser. 407, 27—42, http://dx.doi.org/10.3354/meps08559.

Lavigne, H., D'Ortenzio, F., Ribera D'Alcalá, M., Claustre, H., Sauzède, R., Gacic, M., 2015. On the vertical distribution of the chlorophyll-*a* concentration in the Mediterranean Sea: a basin-scale and seasonal approach. Biogeosciences 12 (16), 5021—5039, http://dx.doi.org/10.5194/bg-12-5021-2015.

L'Helguen, S., Le Corre, P., Madec, C., Morin, P., 2002. New and regenerated production in the Almería-Orán front area, eastern Alboran Sea. Deep-Sea Res. Pt. I 49 (1), 83—99, http://dx.doi.org/10.1016/S0967-0637(01)00044-9.

Lomas, M.W., Lipschultz, F., 2006. Forming the primary nitrite maximum: nitrifyers or phytoplankton? Limnol. Oceanogr. 5 (15), 2453—2467, http://dx.doi.org/10.4319/lo.2006.51.5.2453.

López-Jurado, J.L., Balbín, R., Amengual, B., Aparicio-González, A., Fernández de Puelles, M.L., García-Martínez, M.C., Gaza, M., Jansá, J., Morillas-Kieffer, A., Moya, F., Santiago, R., Serra, M., Vargas-Yáñez, M., Vicente, L., 2015. The RADMED monitoring program: towards an ecosystem approach. Ocean. Sci. 11 (6), 645—671, http://dx.doi.org/10.5194/osd-12-645-2015.

López-Jurado, J.L., García-Lafuente, J., Cano Lucaya, N., 1995. Hydrographic conditions of the Ibiza Channel during November 1990, March 1991 and July 1992. Oceanol. Acta 18 (2), 235—243.

Lorbacher, K., Dommenget, D., Niiler, P.P., Köhl, A., 2006. Ocean mixed layer depth: a subsurface proxy of ocean-atmosphere variability. J. Geophys. Res. 111 (C7), C07010, http://dx.doi.org/10.1029/2003JC002157.

Macias, D., Bruno, M., Echevarnia, F., Vazquez, A., Garcia, C.M., 2008. Meteorologically-induced mesoscale variability of the North-western Alboran Sea (southern Spain) and related biological patterns. Estuar. Coast. Shelf Sci. 78 (2), 250—266, http://dx.doi.org/10.1016/j.ecss.2007.12.008.

Macías, D., García-Gorriz, E., Piroddi, C., Stips, A., 2014. Biogeochemical control of marine productivity in the Mediterranean Sea during the last 50 years. Global Biogechem. Cy. 28 (8), 897—907, http://dx.doi.org/10.1002/2014GB004846.

Macías, D., García-Gorriz, E., Stips, A., 2018. Major fertilization mechanisms for Mediterranean Sea coastal ecosystems. Limnol. Oceanogr. 63 (2), 897—914, http://dx.doi.org/10.1002/lno.10677.

Manca, B., Burca, M., Giorgetti, A., Coatanoan, C., García, M.J., Iona, A., 2004. Physical and biological averaged vertical profiles in the Mediterranean regions. An important tool to trace the climatology of water masses and to validate incoming data from operational oceanography. J. Mar. Syst. 48 (1—4), 83—116, http://dx.doi.org/10.1016/j.jmarsys.2003.11.025.

Marty, J.C., Chiavérini, J., 2010. Hydrological changes in the Ligurian Sea (NW Mediterranean, DYFAMED site) during 1995—2007 and biogeochemical consequences. Biogeosciences 7 (7), 2117—2128, http://dx.doi.org/10.5194/bg-7-2117-2010.

Marty, J.C., Chiavérini, J., 2002. Seasonal and interannual variations in phytoplankton production at DYFAMED time-series station, northwestern Mediterranean Sea. Deep Sea Res. Pt. II 49 (11), 2017—2030, http://dx.doi.org/10.1016/S0967-0645(02)00025-5.

Millot, C., 1999. Circulation in the Western Mediterranean Sea. J. Mar. Syst. 20 (1—4), 423—442, http://dx.doi.org/10.1016/S0924-7963(98)00078-5.

Minas, H.J., Coste, B., Le Corre, P., Minas, M., Raimbault, P., 1991. Biological and geochemical signatures associated with the wáter circulation through the Starit of Gibraltar and the Western Alboran Sea. J. Geophys. Res. 96 (C5), 8755—8771.

Morán, X.A., Estrada, M., 2001. Short-term variability of photosynthetic parameters and particulate and dissolved primary production in the Alboran Sea (SW Mediterranean). Mar. Ecol. Prog. Ser. 212, 53—67, http://www.jstor.org/stable/24864175.

Pai, S.-C., Gong, G.-C., Liu, K.-K., 1993. Determination of dissolved oxygen in seawater by direct spectrophotometry of total iodine.

Mar. Chem. 41 (4), 343—351, http://dx.doi.org/10.1016/0304-4203(93)90266-Q.

Pasqueron de Fommervault, O., Migon, C., D'Ortenzio, F., Ribera d'Alcalà, M., Coppola, L., 2015. Temporal variability of nutrient concentrations in the northwestern Mediterranean sea (DYFAMED time-series station). Deep-Sea Res. Pt. I 100, 1—12, http://dx.doi.org/10.1016/j.dsr.2015.02.006.

Pinot, J.M., Ganachaud, A., 1999. The role of winter intermediate waters in spring-summer circulation of the Balearic Sea: 1. Hydrography and inverse modeling. J. Geophys. Res. 104 (C12), 29843—29864, http://dx.doi.org/10.1029/1999JC900071.

Pinot, J.M., Tintoré, J., Gomis, D., 1995. Multivariate analysis of the surface circulation in the Balearic Sea. Prog. Oceanogr. 36 (4), 345—376, http://dx.doi.org/10.1016/0079-6611(96)00003-1.

Powley, H.R., Cappellen, P.V., Krom, M.D., 2017. Nutrient cycling in the Mediterranean Sea: the key to understanding how the unique marine ecosystem functions and responds to anthropogenic pressures. In: Fuerst-Bjeliš, B. (Ed.), Mediterranean Identities — Environment, Society, Culture. InTech, 47—77, http://dx.doi.org/10.5772/intechopen.70878.

Pujo-Pay, M., Conan, P., Oriol, L., Cornet-Barthaux, V., Falco, C., Ghiglione, J.F., Goyet, C., Moutin, T., Prieur, L., 2011. Integrated survey of elemental stoichiometry (C, N, P) from the western to eastern Mediterranean Sea. Biogeosciences 8 (4), 883—899, http://dx.doi.org/10.5194/bg-8-883-2011.

Ramírez, T., Cortés, D., Mercado, J.M., Vargas-Yáñez, M., Sebastián, M., Liger, E., 2005. Seasonal dynamics of inorganic nutrients and phytoplankton biomass in the NW Alboran Sea. Estuar. Coast. Shelf Sci. 65 (4), 654—670, http://dx.doi.org/10.1016/j.ecss.2005.07.012.

Ravaioli, M., Bergami, C., Riminucci, F., Langone, L., Cardin, V., Di Sarra, A., Aracri, S., Bastianini, M., Bensi, M., Bergamasco, A., Bommarito, C., Borghini, M., Bortoluzzi, G., Bozzano, R., Cantoni, C., Chiggiato, J., Crisafi, E., D'Adamo, R., Durante, S., Fanara, C., Grilli, F., Lipizer, M., Marini, M., Miserocchi, S., Paschini, E., Penna, P., Pensieri, S., Pugnetti, A., Raicich, F., Schroeder, K., Siena, G., Specchiulli, A., Stanghellini, G., Vetrano, A., Crise, A., 2018. The RITMARE Italian fixed-point observatory network (IFON) for marine environmental monitoring: a case study. J. Oper. Oceanogr. 9 (Suppl. 1), s202—s214, http://dx.doi.org/10.1080/1755876X.2015.1114806.

Reul, A., Rodríguez, V., Jiménez-Gómez, F., Blanco, J.M., Bautista, B., Sarhan, T., Guerrero, F., Ruiz, J., García-Lafuente, J., 2005. Variability in the spatio-temporal distribution and size-structure of phytoplankton across an upwelling area in the NW-Alboran Sea (W-Mediterranean). Cont. Shelf Res. 25 (5—6), 589—608, http://dx.doi.org/10.1016/j.csr.2004.09.016.

Ruiz, J., Echevarría, F., Font, J., Ruiz, S., García, E., Blanco, J.M., Jiménez-Gómez, F., Prieto, L., González-Alaminos, A., García, C. M., Cipollini, P., Snaith, H., Bartual, A., Reul, A., Rodríguez, V., 2001. Surface distribution of chlorophyll, particles and gelbstoff in the Atlantic jet of the Alborán Sea: from submesoscale to subinertial scales of variability. J. Mar. Syst. 29 (1—4), 277—292, http://dx.doi.org/10.1016/S0924-7963(01)00020-3.

Sarhan, T., Garcia-Lafuente, J., Vargas, M., Vargas, J.M., Plaza, F., 2000. Upwelling mechanisms in the northwestern Alboran Sea. J. Mar. Syst. 23 (4), 317—331, http://dx.doi.org/10.1016/S0924-7963(99)00068-8.

Schmidtko, S., Stramma, L., Visbeck, M., 2017. Decline in global oceanic content during the past five decades. Nature 542, 335—339, http://dx.doi.org/10.1038/nature21399.

Schroeder, K., Gasparini, G.P., Borghini, M., Cerrati, G., Delfanti, R., 2010. Biogeochemical tracers and fluxes in the Western Mediterranean Sea, spring 2005. J. Mar. Syst. 80 (1—2), 8—24, http://dx.doi.org/10.1016/j.jmarsys.2009.08.002.

Segura-Noguera, M., Cruzado, A., Blasco, D., 2016. The biogeochemistry of nutrients, dissolved oxygen and chlorophyll-*a* in the Catalan Sea (NW Mediterranean Sea). Sci. Mar. 80 (S1), 39—56, http://dx.doi.org/10.3989/scimar.04309.20A.

Sournia, A., 1973. La production primaire planctonique en Méditerranée: Essai de mise à jour. Bulletin de l'Etude en commun de la Méditerranée 5—128.

Strickland, J.D.H., Parsons, T., 1972. A practical handbook of seawater analysis. B. Fish. Res. Board Can. 167, 310 pp., http://dx.doi.org/10.1002/iroh.19700550118.

Tel, E., Balbín, R., Cabanas, J.M., García, M.J., García-Martínez, M. C., González-Pola, C., Lavín, A., López-Jurado, J.L., Rodríguez, C., Ruiz-Villareal, M., Sánchez-Leal, R.F., Vargas-Yáñez, M., Vélez-Belchi, P., 2016. IEOOS: The Spanish Institute of Oceanography Observing System. Ocean Sci. 12 (2), 345—353, http://dx.doi.org/10.5194/os-12-345-2016.

Thingstad, T.F., Krom, M.D., Mantoura, R.F.C., Flaten, G.A.F., Groom, S., Herut, B., Kress, N., Law, C.S., Pasternak, A., Pitta, P., Psarra, S., Rassoulzadegan, F., Tanaka, T., Tselepides, A., Wassmann, P., Woodward, E.M.S., Wexels Riser, C., Zodiatis, G., Zohary, T., 2005. Nature of phosphorus limitation in the ultraoligotrophic Eastern Mediterranean. Science 309, 1068—1071, http://dx.doi.org/10.1126/science.1112632.

Treguer, P., Le Corre, P., 1975. Manuel d'analyse des sels nutritifs dans l'eau de mer, Utilisation de l'AutoAnalyser II Technicon, Occidentale, Vol. 5. Univ. Bretagne, Laboratoire de Chimie Marine, Brest, France, 110 pp.

Vargas-Yáñez, M., García-Martínez, M.C., Moya, F., Balbín, R., López-Jurado, J.L., Serra, M., Zunino, P., Pascual, J., Salat, J., 2017. Updating temperature and salinity mean values and trends in The Western Mediterranean: The RADMED Project. Prog. Oceanogr. 157, 27—46, http://dx.doi.org/10.1016/j.pocean.2017.09.004.

Vargas-Yáñez, M., Zunino, P., Schroeder, K., López-Jurado, J.L., Plaza, F., Serra, M., Castro, C., García-Martínez, M.C., Moya, F., Salat, J., 2012. Extreme western intermediate water formation in winter 2010. J. Mar. Syst. 105—108, 52—59, http://dx.doi.org/10.1016/j.jmarsys.2012.05.010.

Zar, J.H., 1984. Biostatistical Analysis, 2nd ed. Prentice-Hall, Inc., Englewood Cliffs, 718 pp.